TURBOMACHINERY & PUMP SYMPOSIA | HOUSTON, TX
SEPTEMBER 15-17, 2020
SHORT COURSES: SEPTEMBER 14, 2020

Development and Testing of a Supercritical CO_2 Compressor Operating Near the Dome

Stefan D. Cich
Group Leader
Southwest Research Institute
San Antonio, Texas, USA

J. Jeffrey Moore
Institute Engineer
Southwest Research Institute
San Antonio, Texas, USA

Chris Kulhanek
Research Engineer
Southwest Research Institute
San Antonio, Texas, USA

Jason P. Mortzheim
Senior Engineer, Mechanical
GE Global Research
Niskayuna, New York, USA

Stefan Cich is a Group Leader in the Machinery Section at Southwest Research Institute (SwRI) in San Antonio, TX. He holds a B.S. in Aerospace Engineering from the University of Texas at Austin. His professional experience over the last 9 years has been focused around the design, analysis, and development of high pressure equipment and turbomachinery. His first job for two years focused on high pressure hydraulic fracturing equipment. While at SwRI, his main focus has been on various advanced turbines and compressors for a variety of applications. Much of it has been on the development and testing of equipment for use in super critical CO_2 power cycles. This includes multiple 16 MWe turbines, 2.5 MW compressors, 5.5 MW to 55 MW recuperators, and a 2 MW heater along with all the necessary equipment to fully operate a power loop. Through all of this, he has gained experience in various ASME and API codes, design and manufacturing of advanced equipment through advanced manufacturing processes, complex stress and thermal analysis of high temperature and high pressure equipment, and testing and operating procedures of new age power cycles.

Dr. Jeffrey Moore is an Institute Engineer in the Machinery Section at Southwest Research Institute in San Antonio, TX. He holds a B.S., M.S., and Ph.D. in Mechanical Engineering from Texas A&M University. His professional experience over the last 30 years includes engineering and management responsibilities related to centrifugal compressors and gas turbines at Solar Turbines Inc. in San Diego, CA, Dresser-Rand in Olean, NY, and Southwest Research Institute in San Antonio, TX. His interests include advanced power cycles and compression methods, rotordynamics, seals and bearings, computational fluid dynamics, finite element analysis, machine design, controls and aerodynamics. He has authored over 40 technical papers related to turbomachinery and has three patents issued and two pending. Dr. Moore has held positions as the Vanguard Chair of the Structures and Dynamics Committee and Chair of Oil and Gas Committee for IGTI Turbo Expo, and the Associate Editor for the Journal of Tribology. He is also a member of the Turbomachinery Symposium Advisory Committee, the IFToMM International Rotordynamics Conference Committee, and the API 616 and 684 Task Forces. Dr. Moore is the principal investigator of the Apollo program described in this paper.

Mr. Jason Mortzheim is a senior mechanical engineer at the GE Global Research Center in Niskayuna, NY. He has a B.S. in aeronautical engineering from Rensselaer Polytechnic Institute and a M.S. in aerospace engineering from Georgia Institute of Technology. His area of research has been centered on improving fossil power combined cycle plant efficiency including both steam and gas turbines. Mr. Mortzheim initial area of research focused around advanced seal designs where he has held various roles spanning his 19 year professional career. He has utilized computational methods, both commercial CFD and in-house flow solvers, advanced experimental campaigns including industry leading test rig designs, complete to post commercial operation validation to develop state of the art seal technology ranging from brush seals to film riding seals. Mr. Mortzheim is currently the Principal Investigator for DoE contract, EE0007109 related to advanced sCO2 power cycle compression technology and the GE Principal Investigator supporting DoE contract, FE0028979, 10 MWe sCO2 Pilot Plant Test Facility.

ABSTRACT

Supercritical Carbon Dioxide (sCO_2) power cycles are a transformational technology for the energy industry, providing higher thermal efficiency compared to traditional heat-source energy conversion including conventional fossil and alternative energy sources. The novel cycle significantly reduces capital costs due to smaller equipment footprints and design modularity. In addition, it allows for rapid cyclic load and source following to balance solar and wind energy power swings. Recent testing has been performed on a 2.5 MW sCO_2 compressor operating near the dome. Compressing CO_2 is not novel, but mostly at lower vapor pressures, and also at higher pressure and lower temperatures as a liquid. Compression near the dome is a new interest that has many advantages and challenges. The key advantage is the low head requirement when compressing near the CO_2 dome (35°C [95°F] and 8.5 MPa [1,233 psi]). To pressurize from 8.5 MPa (target inlet pressure of power cycle) to 27.0 MPa (3,916 psi), only a single compressor stage is required. This low head requirement means much less power is required to compress and leads to overall increase in thermal efficiency of these various power cycles. This kind of technology could also be used to reduce the power of Enhanced Oil Recovery (EOR) and Carbon Capture Sequestration (CCS) applications.

This type of compression also brings many challenges. A compressor for this application pushes many current technology limits, including but not limited to: bearing technologies, sealing technologies, damping, rotordynamics, compact machinery packaging, and high-density high-speed compression. In addition, when compressing near the CO_2 dome, there are large swings in density for slight changes in temperature. This is a unique challenge not observed when CO_2 is pumped or compressed as a liquid or vapor. Due to these large changes in density, range extension is required to maintain high compression efficiency and controlled mass flow over a range of operating temperatures. This particular compressor will utilize actuated inlet guides vanes (IGVs) and represents the highest density centrifugal compressor reported in the literature with densities over 60% of water.

INTRODUCTION

This lecture will go over many of the challenges that were encountered during the design and development of this particular compressor. Some of the specific challenges were focused on compressor flow range enhancement and on rotordynamics by managing critical speeds and separation margins. For power applications, the turbine requires near constant mass flow to maintain desired power output. Ambient temperature swings (both daily and seasonal) result in large density swings as shown in Figure 1. Therefore, the volume flow can vary by over a factor of two while operating the compressor at constant speed. To account for the required flow range and turndown, actuated IGVs were incorporated into the design.

The other unique challenge of this application is the high density of CO_2 near the dome, where the density exceeds 600 kg/m^3 (37.5 lbm/ft^3) (60% of water), and represents the highest density compressor reported in literature. Due to its high speed and high density flow, this compressor is outside the range of experience on the Fulton Chart when looking at Critical Speed Ratio (CSR) vs Average Gas Density, Figure 2. This required some unconventional rotor layouts in terms of bearing location, balance piston location, and overall rotor span. The goal of this compressor design was to package a back to back compressor in a single casing. This presented a challenge in overall rotor span and pressure containment of the various stages. In addition to the large pressure differential across the compressor stages, an actuated IGV system was packaged to allow for range extension of the compressor.

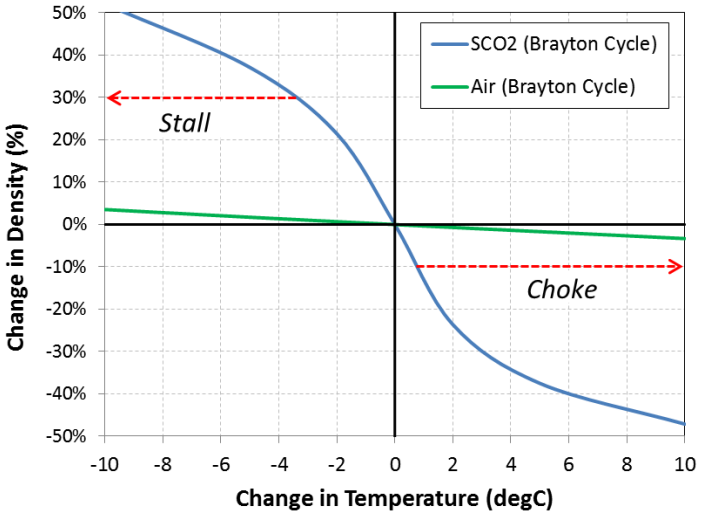

Figure 1 - sCO_2 Density Change vs Temperature near the Dome

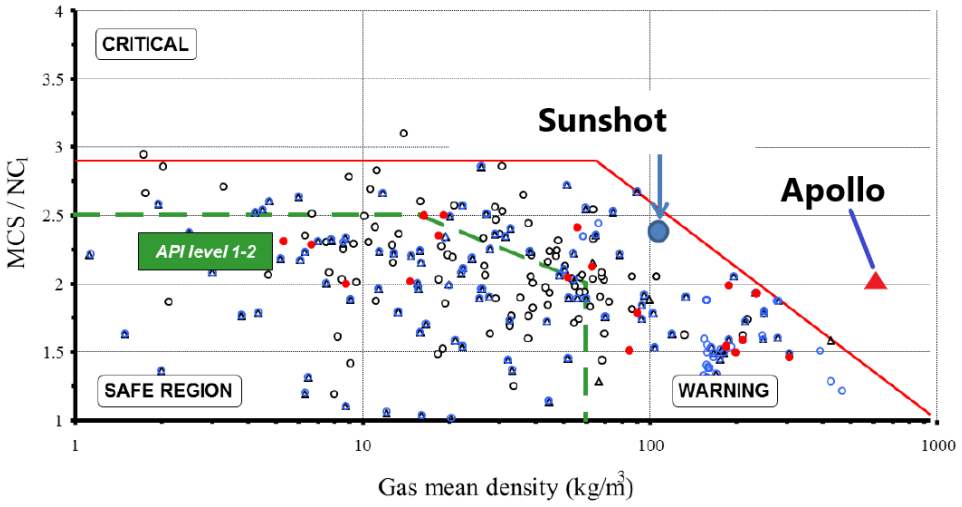

Figure 2. Rotordynamic Experience Chart from [1] with Sunshot Turbine and Apollo Compressor Rotor Added

The program which this sCO_2 compressor was developed under was focused on the development of a Recompression Brayton Cycle (RCBC) for use with Concentrated Solar Power (CSP) technologies. Some of the components and operating conditions are unique to this power cycle, but many of the advantages and challenges for the use of a sCO_2 compressor in this power cycle are also applicable to the use of this technology for other applications, including CCS and EOR. The RCBC is an attractive cycle for sCO_2 that could meet the relative efficiencies of steam based Rankine cycles. To meet these efficiencies, the cycle requires low and high temperature recuperators, turbine inlet temperatures between 600-760ºC (1,112-1,400ºF), a main compressor, and a bypass compressor. There is an ideal balance between the flow split on the main compressor and bypass compressor. While the lower temperature flow requires less power to compress, the higher temperature will increase the effectiveness of the recuperation in the loop [2]-[5]. Other US DOE projects have focused on the cost and effectiveness of the recuperators and the design and development of the high temperature sCO_2 turbine [6]-[8]. The US DOE Apollo program's main focus is on the design and testing of the main compressor for this RCBC. Figure 3 shows the overall cycle model and design conditions that are required for this machinery.

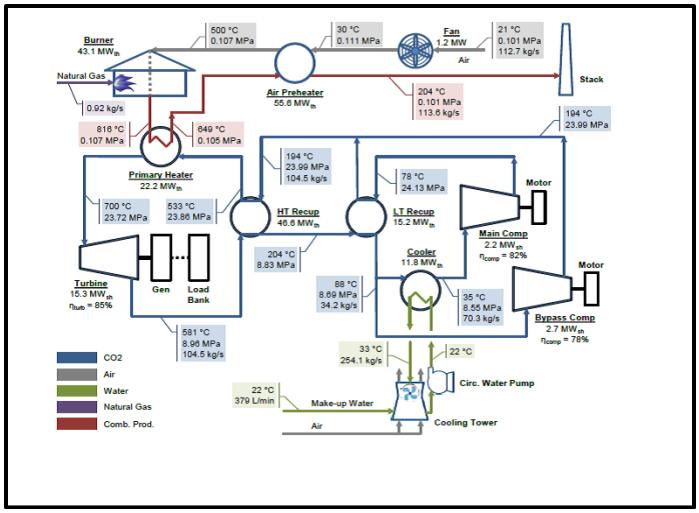

Figure 3 - Proposed Recompression Brayton Cycle with sCO_2

The main compressor has a nominal operating point of 35ºC (95ºF) and 86.9 bar (1,260 psi). This design point is chosen as one of the optimal points for the RCBC due to its effect on the overall cycle efficiency. It is also above the critical point of CO_2 to avoid compressing liquid in the main compressor. Previous papers have reviewed and gone into the detail on compressor design limits with CO_2 and the advantage of compressing in the supercritical state rather than trying to pump in the liquid state [9]-[13]. In terms of overall cycle efficiency, it is important to understand a few characteristics of CO_2 near the dome that are being looked at for the RCBC. This includes average gas density, required head, and required heat rejection to achieve suction conditions varying from 10ºC (50ºF) to 88ºC (190ºF) as shown in Figure 4 and Figure 5. Depending on the application, the optimum suction temperature will vary. For CCS and EOR, the

goal will be to stay to the right of the CO_2 dome as shown in Figure 6. Staying to the right of the dome will avoid the potential for two phase compression of CO_2 liquid and vapor and also require less cooling to achieve higher downhole pressures.

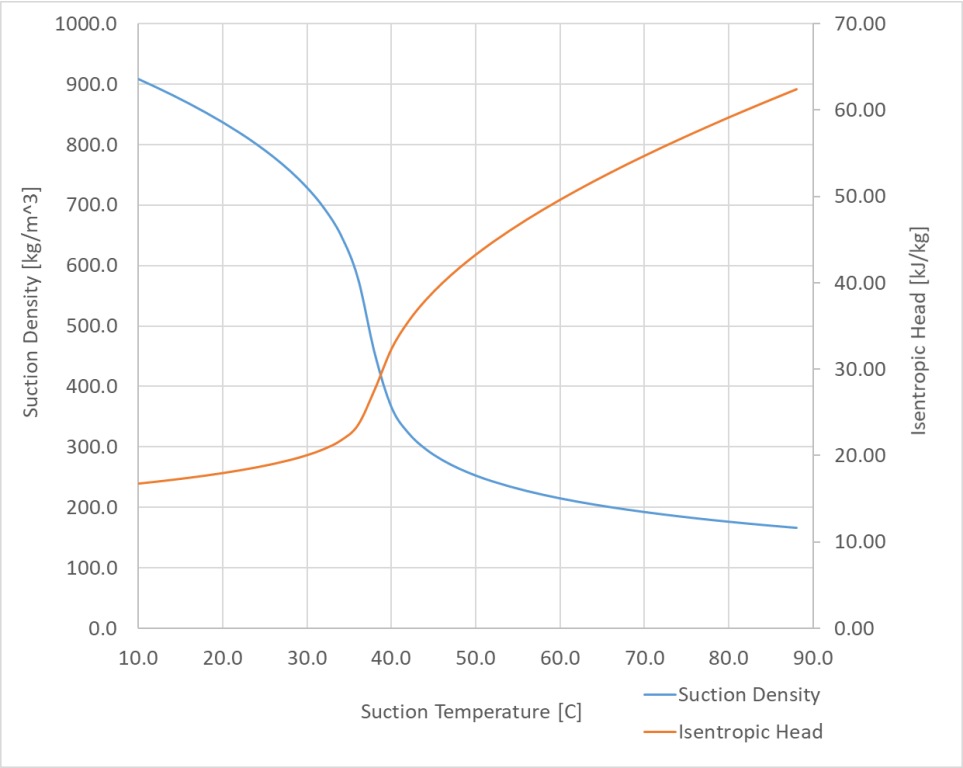

Figure 4 - Suction Density and Isentropic Head vs Suction Temperature

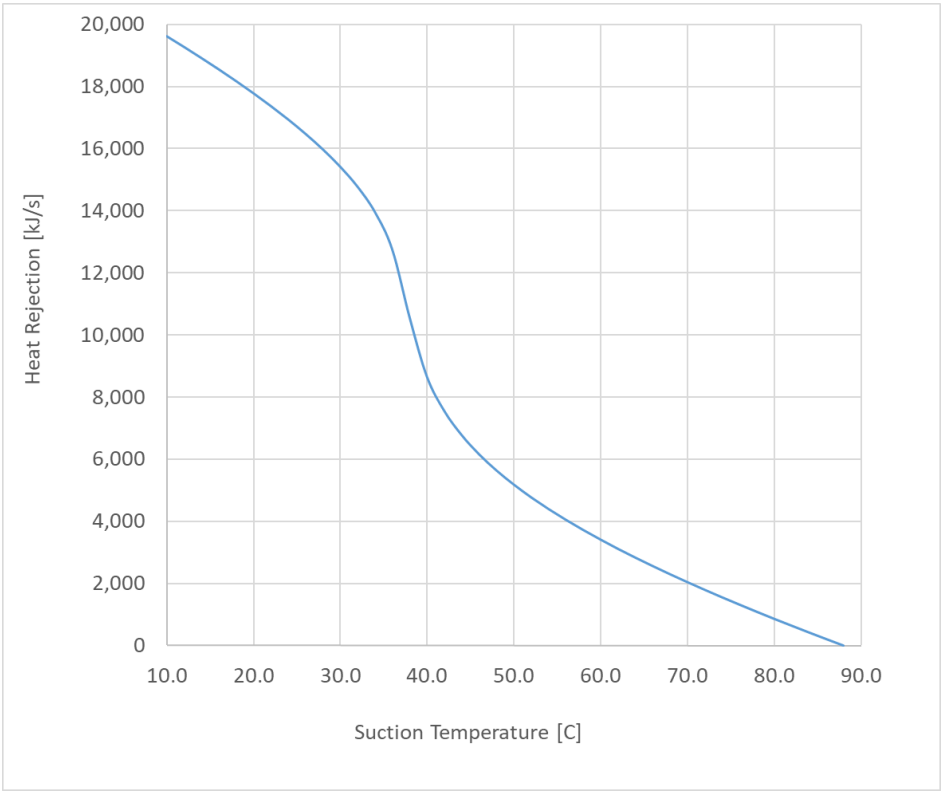

Figure 5 - Heat Rejection vs Suction Temperature

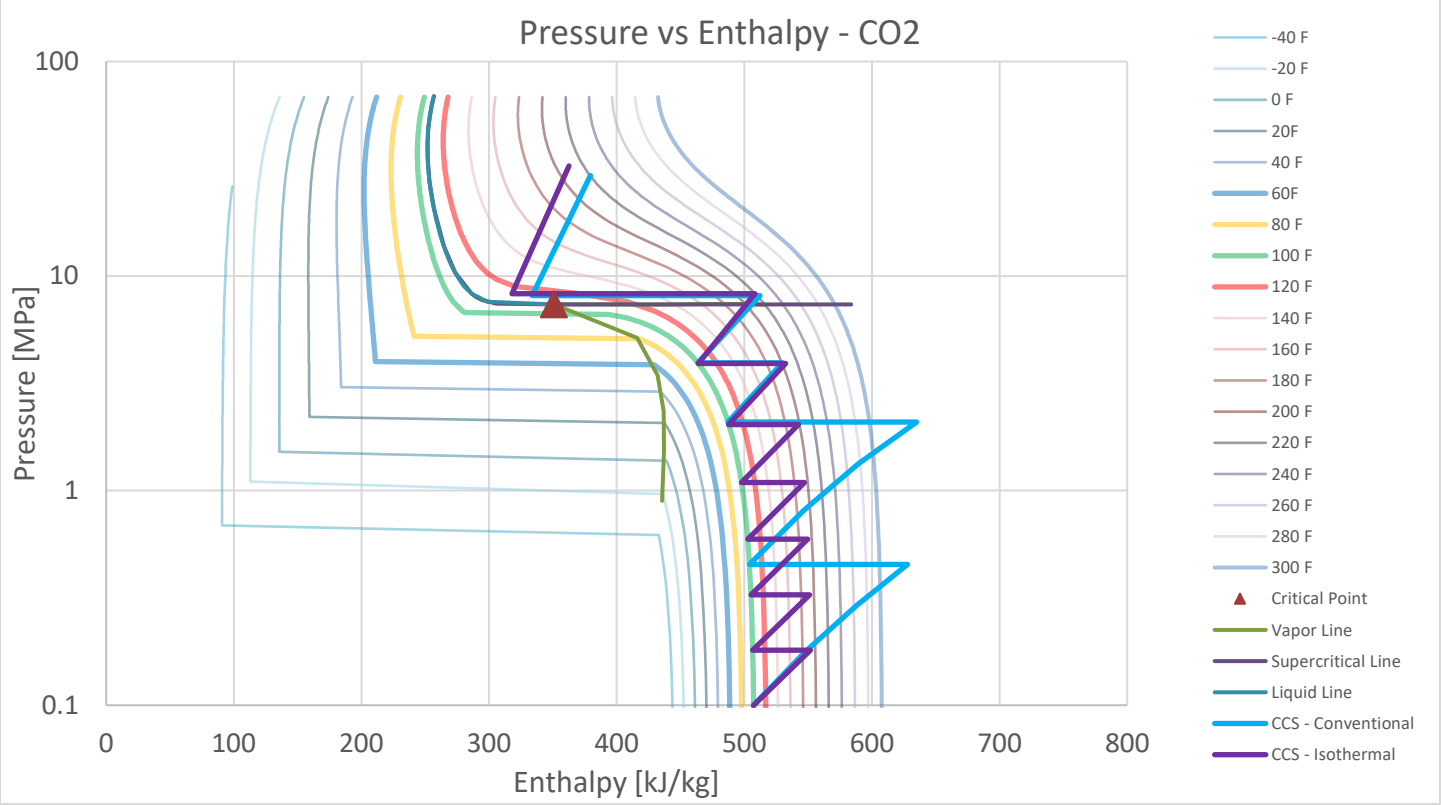

Figure 6 - Semi-Isothermal Compression vs Conventional Compression

For power cycle efficiency and required power to compress CO_2, it is important to understand compression power (head requirement) and heat rejection needed to achieve the target suction temperature. What can be seen is that for cooler suction flows, the head requirement reduced. There is an inflection point around 35ºC (95ºF) where head requirement for sCO_2 compression are similar to liquid CO_2. However, there is also an inflection point around 35ºC (95ºF) for the amount of heat rejection needed to achieve those suction conditions. Total required power is based on compression head and required heat rejection. If using dry cooling with air or evaporative cooling with cooling water, the power required for heat rejection is based on the air blowers or water pumps. This means heat rejection is relatively cheap down to a certain temperature. If additional chilling is required, more power is required to achieve the colder suction temperatures.

Because of these cooling requirements, to goal suction temperature range 20ºC (68ºF) (pure liquid) to 50ºC (122ºF) [14]. This is based on minimum and maximum atmospheric temperatures in various regions around the world and how much heat can be rejected through dry cooling or evaporative cooling. As seen in Figure 4, this means a compressor has to be designed to operate over a wide range of densities while supplying near constant mass flows. Based on various operating temperatures, there is an optimal split between the main and the bypass compressor. With this 3X swing in density, there would also be a 3X swing in volume flow. In order to maintain high compression efficiency, this requires the need for active flow control, and variable IGVs were chosen for this application [15][16].

Density has a significant effect on rotordynamic behavior due to its effect on fluid forces. This is shown in Figure 2 in the Fulton Chart comparing API requirements and experience in terms of CSR vs average gas density. One approach to deal with the high average gas density would be to operate a sub critical machine. CSR is the ratio of max continuous operating speed (MCOS) to the 1st undamped rotor mode. A sub critical machine has a CSR less than 1.0, which is represented by points below the Fulton Chart in Figure 2. Operation below a CSR of 1.0 will either be a short and stiff rotor at high speed, or a lower speed shaft. For these relative densities, the usual choice would be a low speed dense phase liquid pump, however, when looking at required cooling, this leads to a negative effect on overall efficiency, and will also lead to a much larger machine with more stages and increased secondary losses. By being able to compress in the supercritical phase, a high speed, high efficiency single stage wheel can be utilized to reduce the overall power required.

One of the unique challenges of this design and application, and the reason why the rotor is operating at a high CSR is because it was designed to package both the main compressor and bypass compressor in a single case. For this power cycle, by having both compressors packaged in a single case and also speed matched to the turbine, a directly coupled train could be designed that would reduce the overall footprint of the 10 MWe power block. This configuration is not ideal for other applications unless extreme pressures or higher flows are needed in which a two stage back to back sCO_2 compressor would be advantageous. A back to back design of this nature would be ideal for a two stage CO_2 compressor at lower pressures, but those speeds would be much lower along with lower fluid forces that will be comparable to what is seen in initial low pressure testing of this compressor. This paper will take a detailed look at the mechanical design

and testing of the compressor and will not focus on the aerodynamic performance. This will be focused on in other papers as testing is completed and full compressor maps are developed.

ROTORDYNAMIC DESIGN

The previous paper that discussed the design of this compressor highlighted some of the necessary rotor features, which included journal bearings, hole pattern seals, and thrust bearings. For this application, similar to the design of a sCO_2 Turbine [6], Integral Squeeze Film Damper (ISFD) bearings were chosen to improve rotordynamic performance [17]. At that time, the rotor design was based on a more conventional approach as shown in Figure 7 and Figure 8, but due to design margin with the 3rd mode, the rotor layout was changed to create more separation margin between operating speed and the calculated modes. Configuration 1 has a separation margin of only 1.3%. This configuration had a more standard design in which the thrust collar was outboard of the journal bearing on the non-drive end (NDE) of the rotor, the coupling was outboard of the journal bearing on the drive-end (DE) of the rotor, dry gas seals (DGS) were directly inboard of the journal bearings, and the balance piston was between the bypass compressor suction and the DE DGS. Even though this compressor was a back to back design, a balance piston was needed to account for off design scenarios since there was potential for the use of only the main compressor. In addition, since these compressors were discharging to different points in the loop along with different suction conditions, there would be slight differences in pressure rise across each compressor during standard operation that could lead to thrust imbalance.

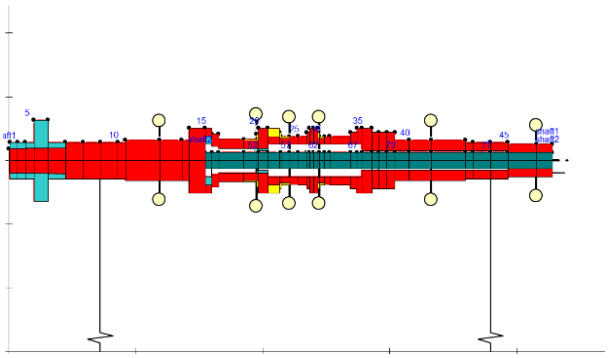

Figure 7 - Rotor Layout - Configuration 1

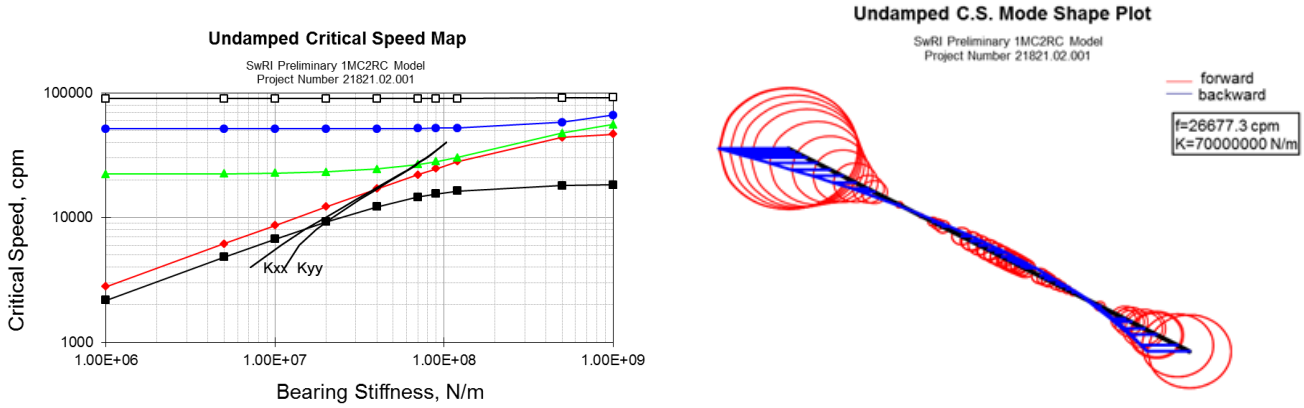

Figure 8 - Undamped Criticial Speed Map (Left) and 3rd Mode (Right) with 1.3% separation margin for Configuration 1

To improve this separation margin, the balance piston was moved in between the main compressor and bypass compressor to allow for significant damping in the middle of the rotor. Due to the high pressure drop, mass flow, and density across the balance piston that is unique for sCO_2 compression, the balance piston is beneficial to the overall stability of the machine. This is why a hole pattern damper seal is used rather than a labyrinth seal. One disadvantage though, is that a hole pattern seal requires larger clearances, especially in the middle of the rotor where motion would have the highest amplitude, which leads to more mass flow through the seal and a direct impact on overall efficiency. This configuration is shown in Figure 9. With increased damping, the mode only dropped by 500 cpm, increasing separation margin to 3.1%, with operation still above the 3rd mode.

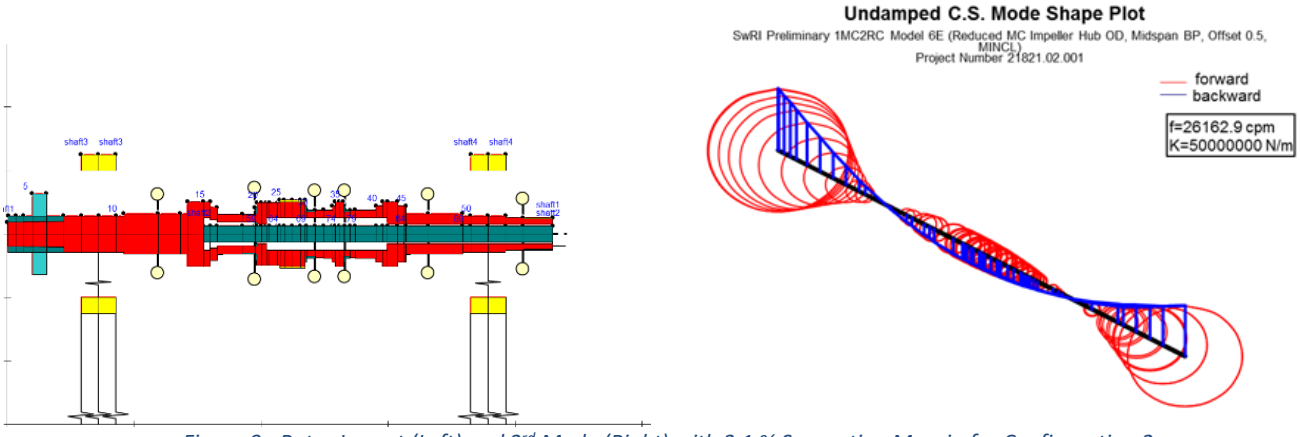

Figure 9 - Rotor Layout (Left) and 3rd Mode (Right) with 3.1 % Separation Margin for Configuration 2

For Configuration 3, Figure 10, the thrust bearing was moved inboard of the journal bearing due to a nodal point of the mode acting right at the journal bearing location. By moving the thrust bearing inboard and increasing the bearing span, the margin to the 3rd mode was increased. In addition to increasing the span, moving the thrust bearing inboard also reduced the overhung moment on the Non-Drive End (NDE) of the compressor, therefore increasing the 3rd mode. The main disadvantage of this approach is that journal bearing sizes are limited. For a small rotor like this, the static loads on the bearings are small, but larger bearings could provide more stiffness that would assist in limiting motion of the rotor with the potential for high vibrations due to the high density flow and high speed operation.

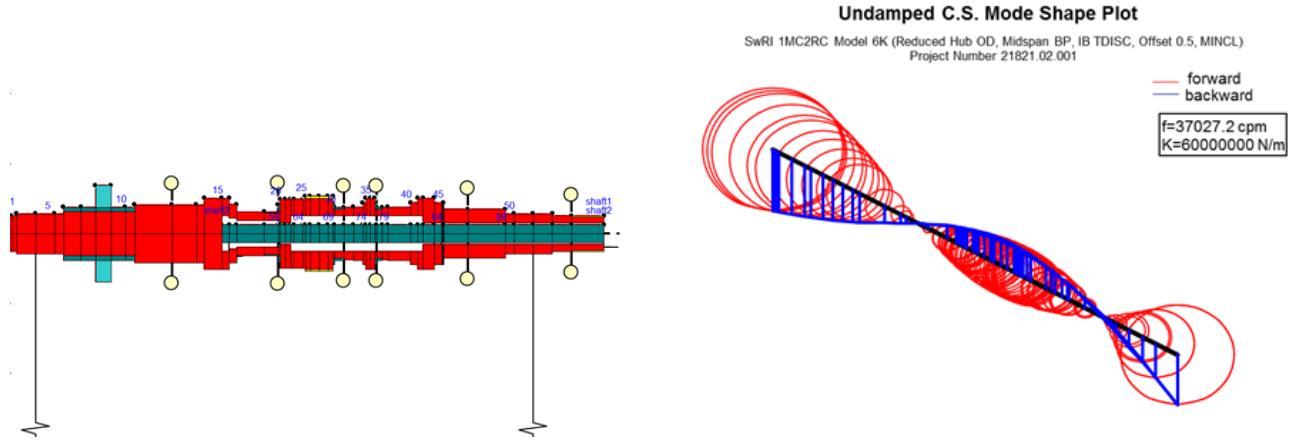

Figure 10 - Rotor Layout (Left) and 3rd Mode (Right) with 37% Separation Margin for Configuration 3

By moving the thrust bearing inboard, the 3rd mode was increased significantly (37% margin). This allows for significant separation margin to operating speed and led to the final rotor configuration for this design. One of the challenges with moving the thrust bearing inboard is that some significant design changes were required for the original thrust bearing and thrust collar. By keeping the bearings the same size, the minimum diameter of the thrust collar was increased to be larger than the bearing diameter, rather than the largest diameter of the thrust collar taper being at the bearing diameter. This also prevents the potential of increasing bearing sizes if more stiffness is needed. Due to the current design envelope, the same size thrust bearing would have to be used to keep the same outer diameter and also the same required oil flow. In order to account for a larger diameter thrust collar, the thrust bearing inner diameter was increased, therefore decreasing the thrust capacity of the thrust bearing. This change reduced the overall thrust capacity by around 15%, but in terms of total thrust the rotor could be seeing without a balance piston, the change is minimal. When operating with a high pressure compressor, thrust position and thrust bearing RTDs will be evaluated closely during initial start-up to ensure proper thrust balance.

Figure 11 shows the final cross-section of the compressor. The compressor was designed as a back-to-back concept accommodating both the main and bypass compressor in the sCO_2 RCBC. However, for the initial testing, only the main compressor impeller was implemented and the two recompressor impellers are represented as simple disks to capture the impact on rotordynamic behavior. The barrel design uses a modular bundle that can be installed and removed from the case as an assembly to simplify installation and maintenance. The bundle utilizes non-split diaphragms made possible with the modular rotor construction with a central tie-bolt. The main compressor diaphragm must support 17.0 MPa (2,466 psi) pressure differential and contain the variable IGVs. Due to the relative small diameter of the main impeller, the hub diameter at the impeller is smaller than the dry gas seal diameter, which is driven by the

journal bearing, coupling, and inboard thrust bearing arrangement, making a traditional shrunk-on impeller impossible without unacceptably poor rotordynamic behavior. The modular assembly solves this design challenge while maximizing rotor diameter along the shaft. In order to improve the structural integrity of this high density impeller, a 5-axis electrode discharge machining (EDM) was utilized in its manufacturing followed by extrude-honing to improve surface finish resulting in a single-piece part (no welding or brazing).

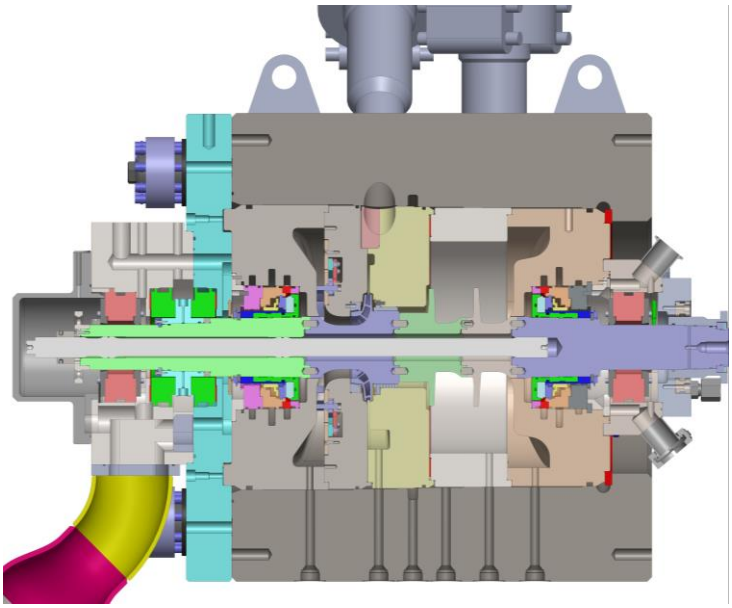

Figure 11 - Apollo Compressor Cross-section

COMPRESSOR CONSTRUCTION

To achieve a well-balanced and tight runout rotor, all components were manufactured and balanced individually first. All critical faces (bearing locations, thrust collar, balance piston, and DGS mounting surfaces) had extra stock that could be ground down as a completed assembly to ensure tight runout tolerances typical of a high speed shaft could be maintained. After grinding was completed, the entire assembly went through a low speed balance to meet API 684 G2.5 requirements. Figure 12 shows the final assembled rotor. "Ping" tests were conducted to verify the rotor free-free natural frequencies and mode shapes to be compared to analytical model predictions. Because of the built up rotor configuration, balance planes are accessible on both ends of the machine to allow for high speed trim balancing during initial start-up and testing of the compressor along with additional testing after disassembly.

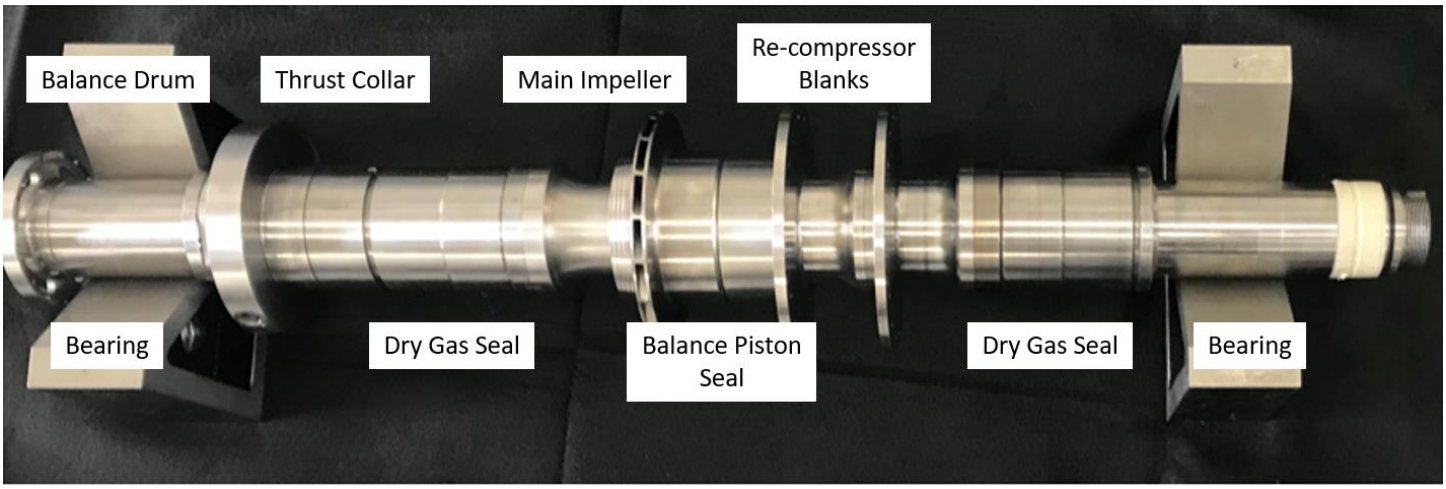

Figure 12 - Assembled Compressor Rotor

As previously mentioned, variable IGVs are utilized to greatly increase the flow range and off-design efficiency of the compressor. These are shown in Figure 13 at the +10° (left) and -60° (right) positions. An external actuator with a pressure seal through the case is used to vary to IGV position and can be done in real time while the compressor is operating.

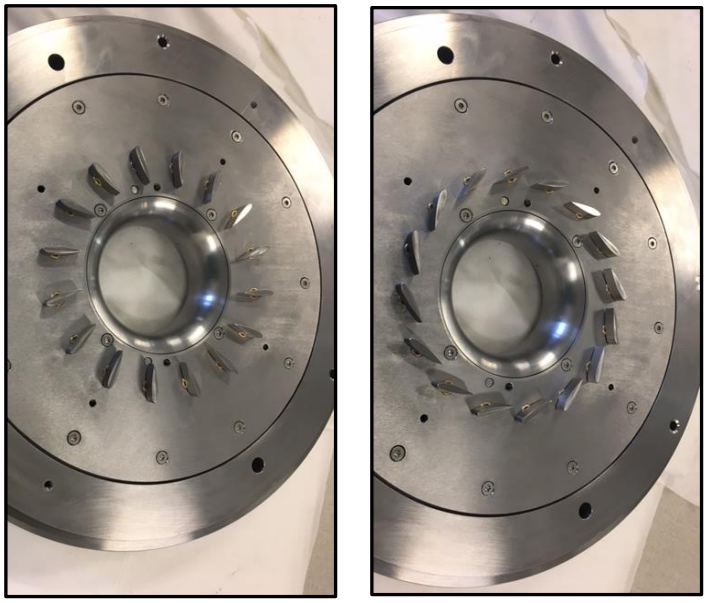

Figure 13 - Actuated IGVs for Range Extension

Figure 14 shows the final assembled compressor on the test stand. The compressor was mated to the existing sCO_2 test loop at SwRI. The lube oil system supply and drains, dry gas seal supply and vent, and separation (buffer) air connections were made. The compressor is driven by a 3 MW, 1800 rpm motor with two speed increasing gearboxes allowing speeds up to 28,350 rpm (105%).

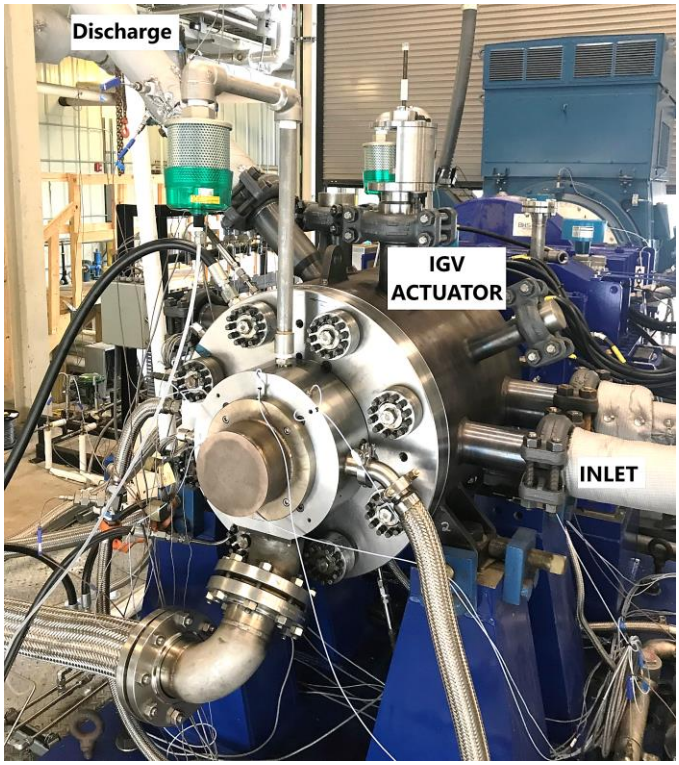

Figure 14 - 2.5 MW sCO_2 Compressor Test Stand at SwRI

LOW PRESSURE TESTING

Based on experience from previous testing the test plan for this compressor was developed to run the compressor at low pressure operating conditions first, 0.3 and 2.0 MPa, to check the mechanical integrity of the machine [18]. By running at lower pressures, the fluid forces are reduced on the impeller and seals that could lead to issues in mechanical performance. This allows the focus of the

testing to be on control of the system and the mechanical integrity of the machine. By mechanical integrity, the focus will be on rotor vibrations in the compressor, overall vibrations in the motor and gearbox at low load conditions, bearing temperatures in the compressor, verification of all instrumentation, and verification of all performance calculations. This allows for low risk testing and for the system to be evaluated to make sure everything is operating and reading correctly before high risk conditions are reached. This ensures that trips are working properly for the overall safety of the system, performance calculations are accurate, and verification of proper operation of auxiliary systems. Test results for the first test up to speed are shown in Figure 15 and Figure 16 with a focus on the bearing vibrations and bearing temperatures. These are the two most important measurements to look at when first running up to speed to ensure there is no issue in the rotor stack and rotor balance.

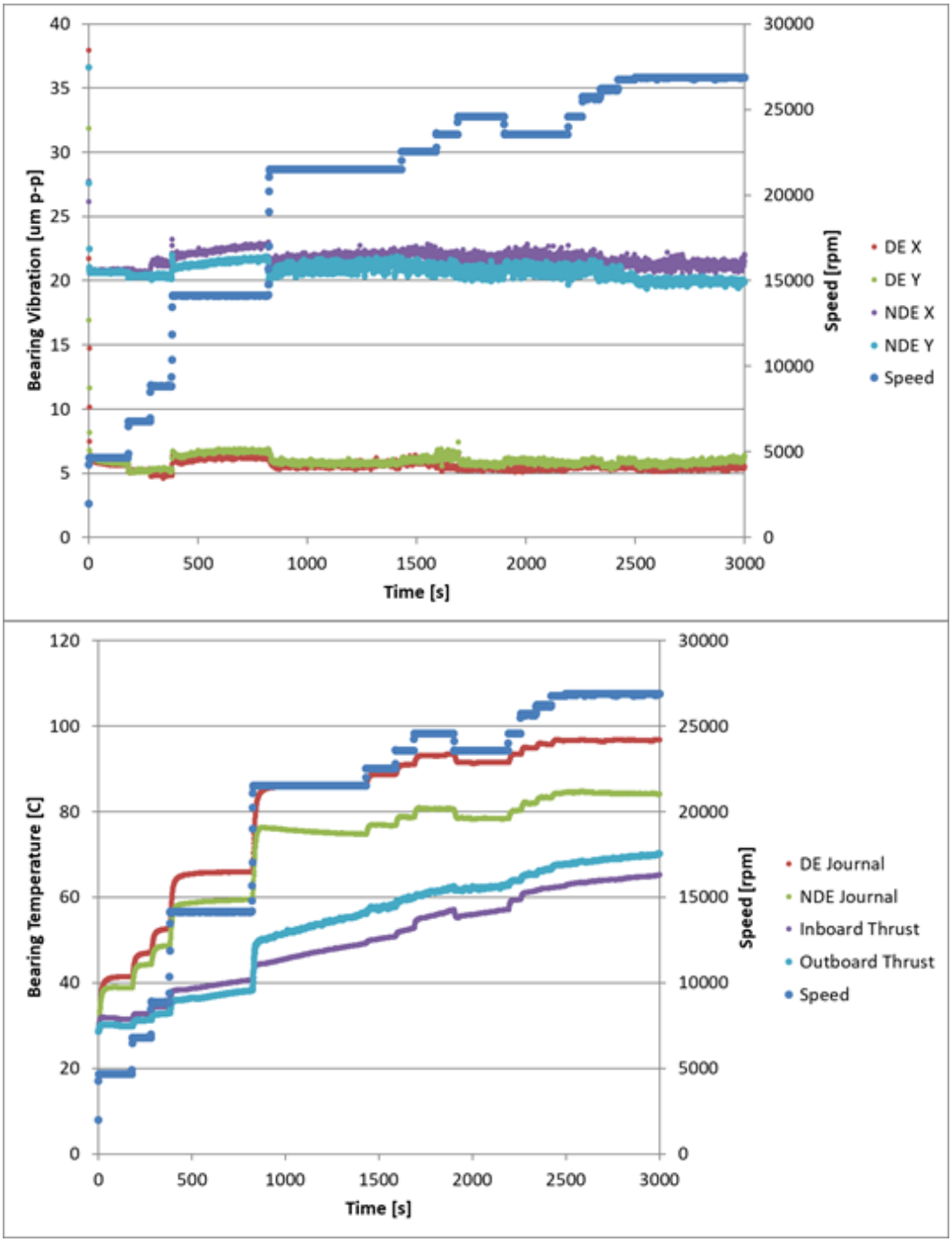

Figure 15 - First Test to Full Speed - Bearing Vibrations (top) and Bearing Temperatures (bottom)

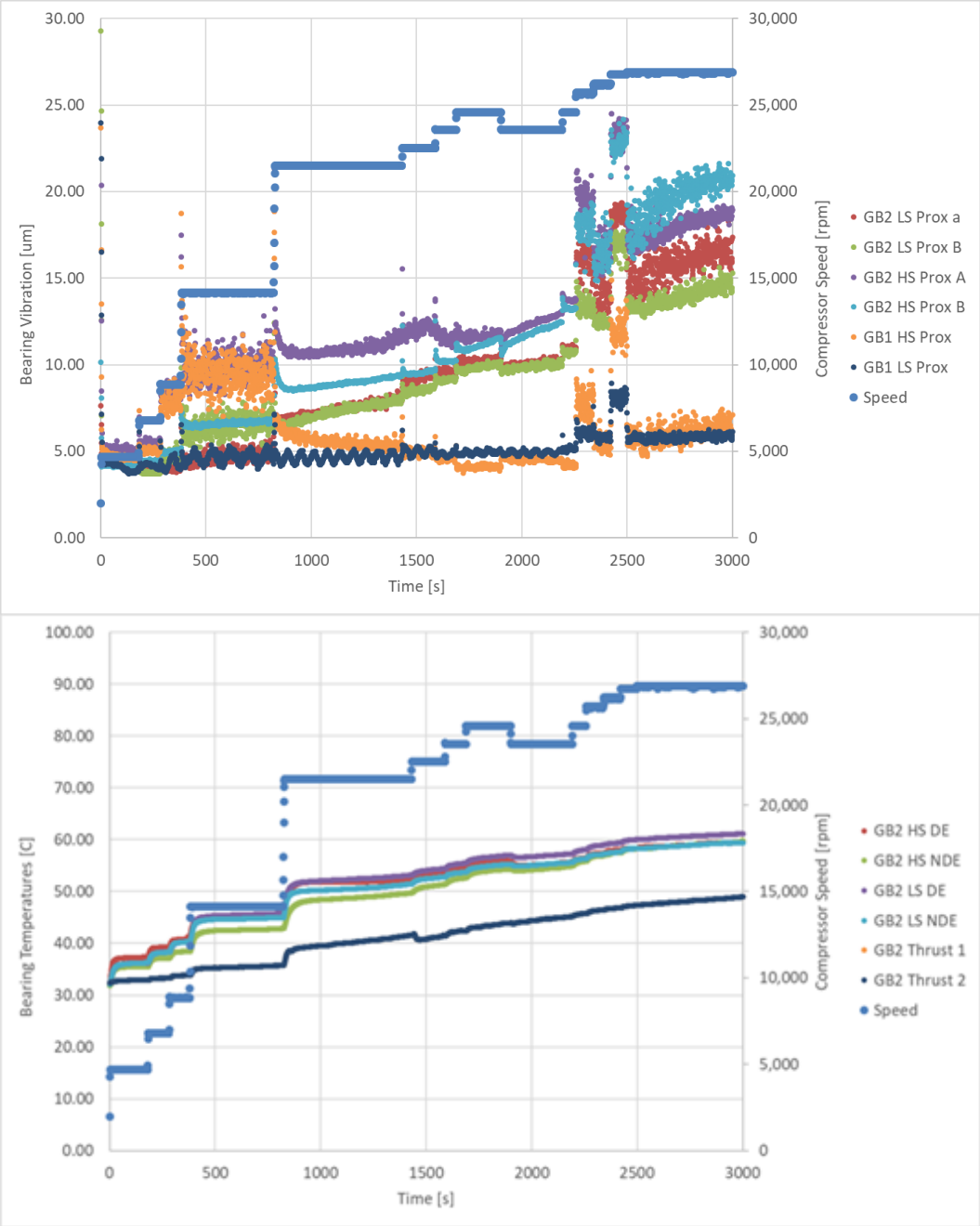

Figure 16 - First Test to Full Speed - Gearbox Bearing Vibrations (top) and Temperatures (bottom)

As can been seen in the above figures, the first time the compressor was brought up to full speed, the ramp up procedure was slow and in small steps to make sure everything was working properly and as expected. The bearing temperatures are level and the bearing vibrations are below design limits. For this testing, bearing vibration limits were set to alarm at 35.5 µm (1.4 mils) and to trip at 43.1 µm (1.7 mils) for the compressor.

Low bearing temperatures and low vibrations indicate the bearing clearances are sufficient and the bearings will not be damaged due to excessive running temperatures at full speed. This applies to the journal and the thrust bearings. For both sets of bearings, the alarm is set at 120ºC (248ºF) and to trip at 135ºC (275ºF). Peak temperatures were around 110ºC (230ºF) which indicates no tight running bearings and also sufficient cooling in the lube oil system. In terms of vibration, at low pressures the destabilizing fluid forces that could excite rotordynamic modes are low. The peak vibrations were less than 25 um (1 mil) indicating good rotor balance, and there was no need to trim balance the rotor. With a built up rotor as used in this machine, it is important to perform a low balance check after every assembly to ensure that everything is properly seated and in the right orientation.

After maximum speed was achieved at low pressure, the next step in the test procedure was to go up to speed at a medium pressure (2.0 MPa [300 psi]) and obtain compressor maps at various speeds and IGV settings with ideal gas (away from the liquid-vapor dome). One of the complications with compressing sCO_2 near the dome is the uncertainty of performance with real gas effects that will need to be confirmed by comparing CFD results and performance data. Operating data is shown in Figure 17 and Figure 18. In addition to bearing vibrations and temperatures compared to speed, this data also takes a look at fluid density effects. From 0.3 to 2.0 MPa, the density is increased by around 7X, which increases potential excitations from fluid forces. Also, with the higher pressure loads, it is important to look at thrust bearing temperatures to ensure that thrust predictions are accurate.

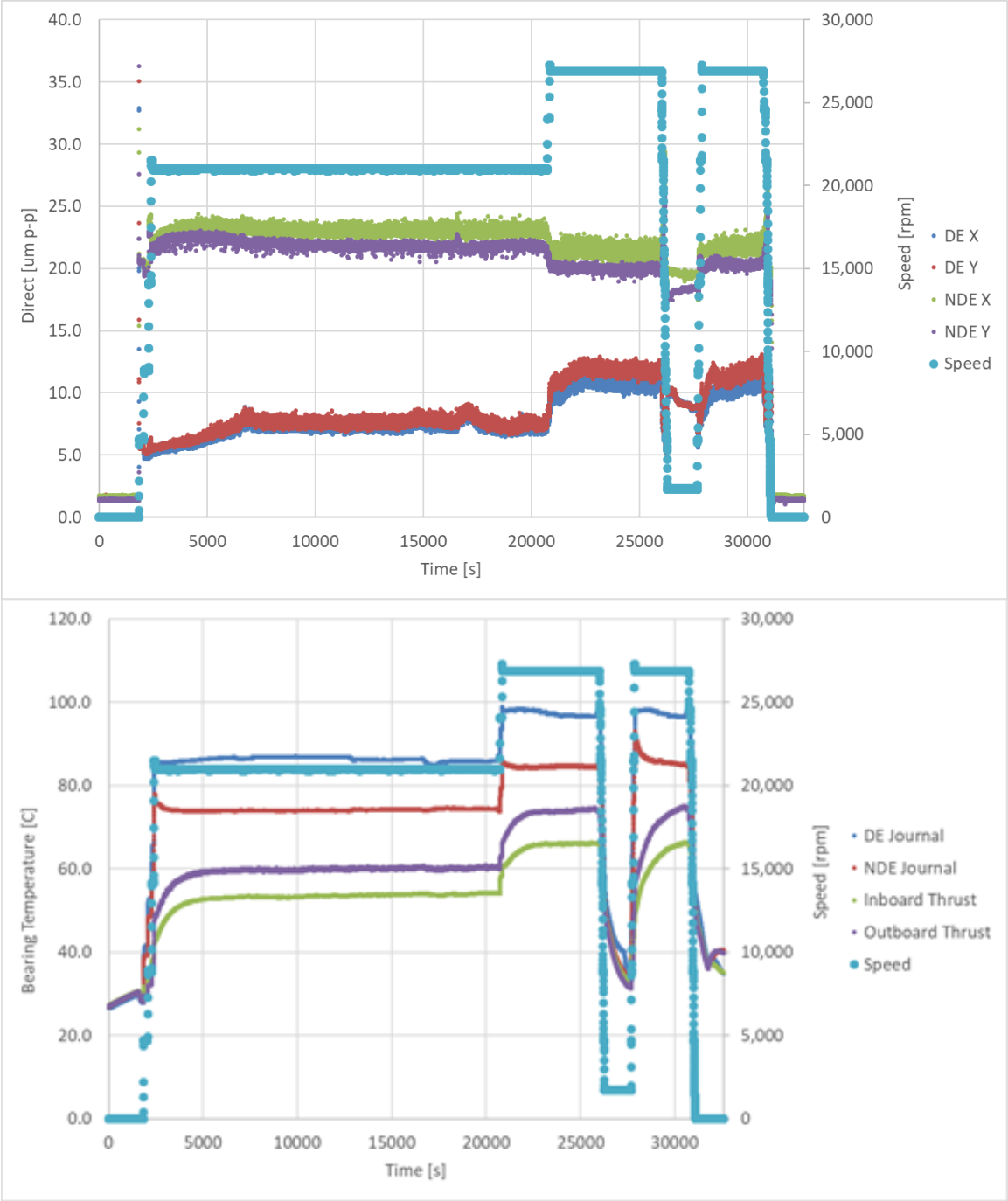

Figure 17 – 2.0 MPa Test - Bearing Vibrations (top) and Bearing Temperatures (bottom) Compared to Speed

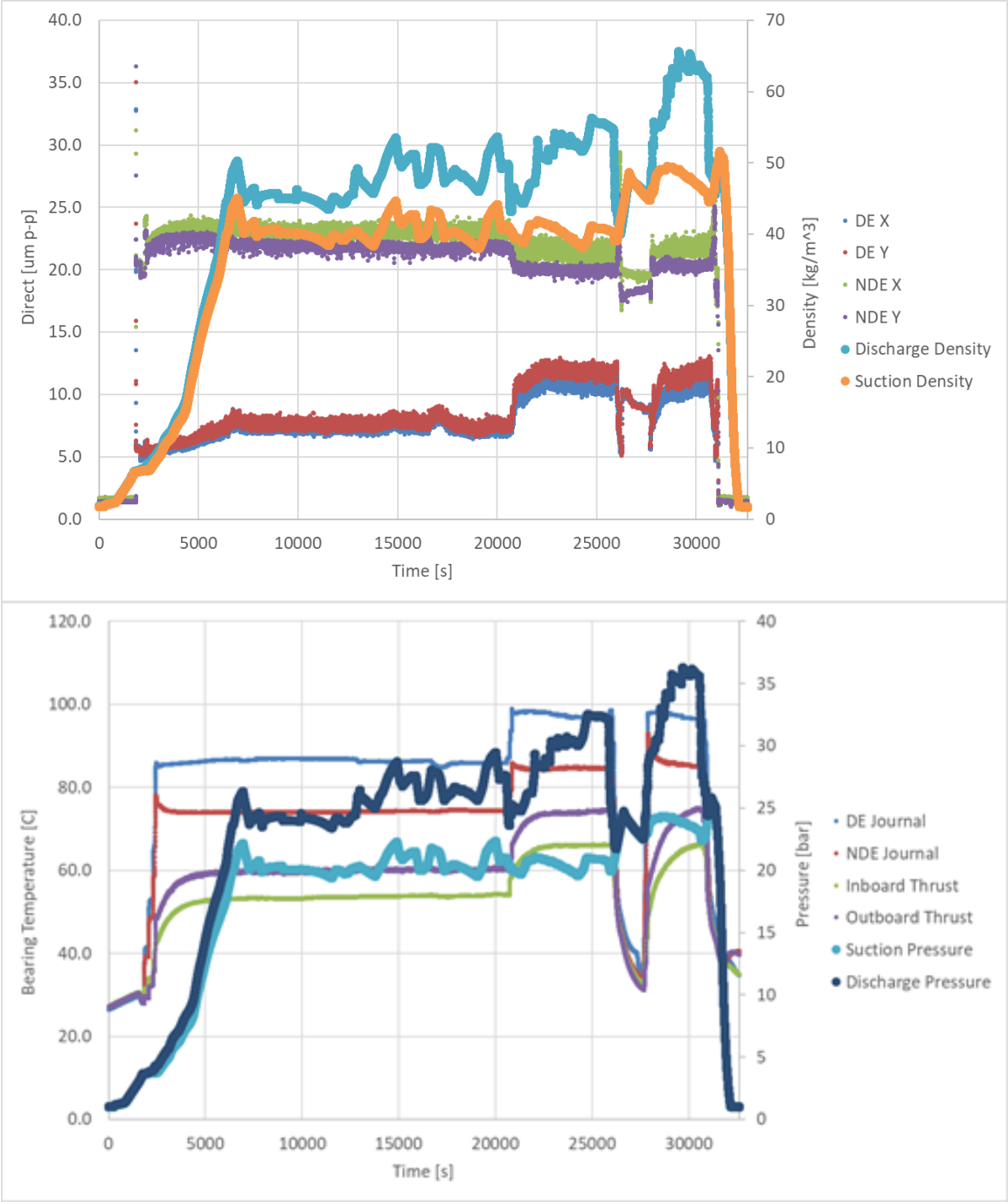

Figure 18 – 2.0 MPa Test - Bearing Vibrations and Flow Density (top) and Bearing Temperature and Fluid Pressures (bottom)

It is important to note that these above tests were performed without any disassembly of the compressor. With higher pressures and operating densities, the bearing vibrations were monitored as the compressor is sped up, but the compressor can be ramped up quicker than initial testing. When comparing the two tests, the vibrations on the NDE bearings are very close, 22 um vs 23 um (<1 mil). For the Drive End (DE) bearings, the vibrations are doubled between the two tests, 5 um (0.2 mils) vs 10 um (0.4 mils). It is also noticeable that as the compressor is throttled and discharge densities are increased, the NDE bearing vibrations appear to increase. This indicates some effect of fluid density on the stability of the rotor, but it is not fully understood what the root cause is. Potential areas where increased fluid density and pressure can lead to an impact on rotor dynamic stability are: flow across the balance piston, pressure loads from the volute, flow instabilities off the IGVs, and flow through the impeller. Overall, all of the vibrations and temperatures are still operating as expected and there is no indication of any rotordynamic instability of concern. Densities at these conditions are around 10% of the density at maximum operating conditions. Detailed vibration plots are shown in Figure 19 through Figure 21.

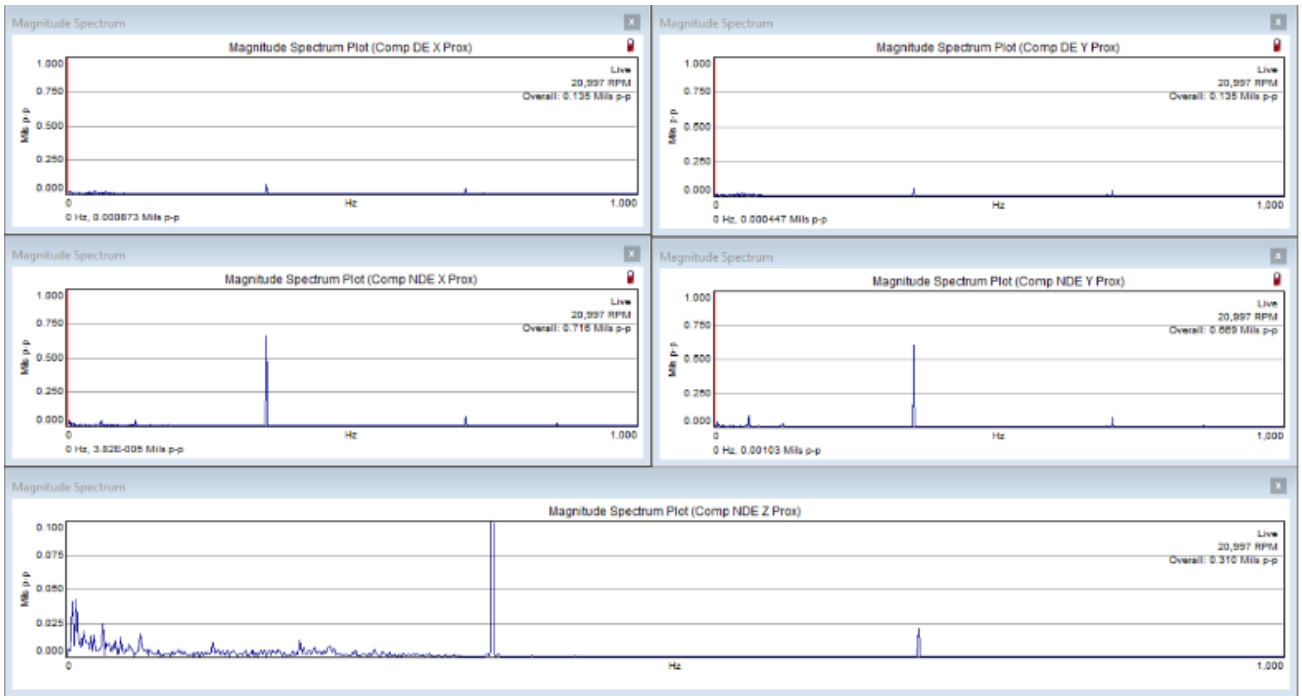

Figure 19 – 2.0 MPa Test - Vibration Plots at 21,000 rpm at +10 IGV Set Point

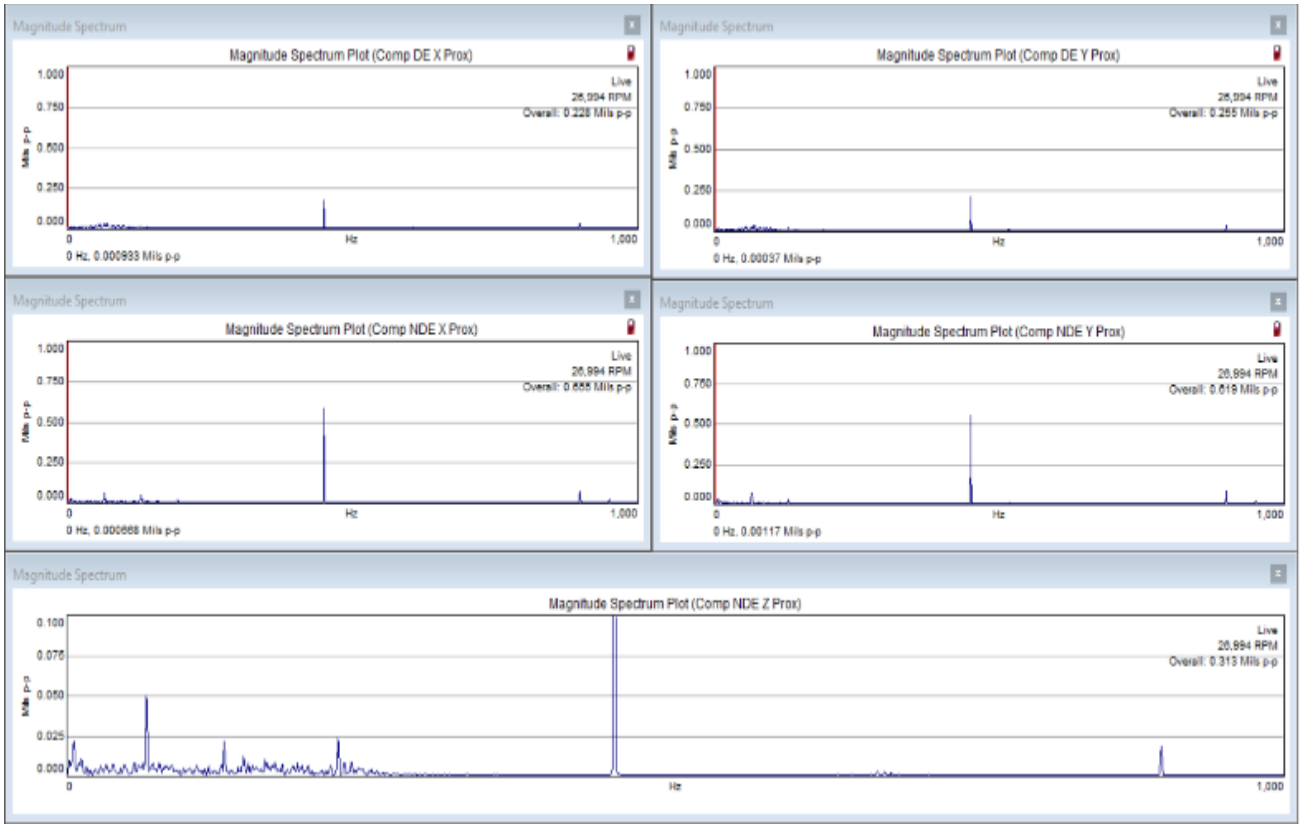

Figure 20 – 2.0 MPa Test - Vibration Plots at 27,000 rpm at +10 IGV Set Point

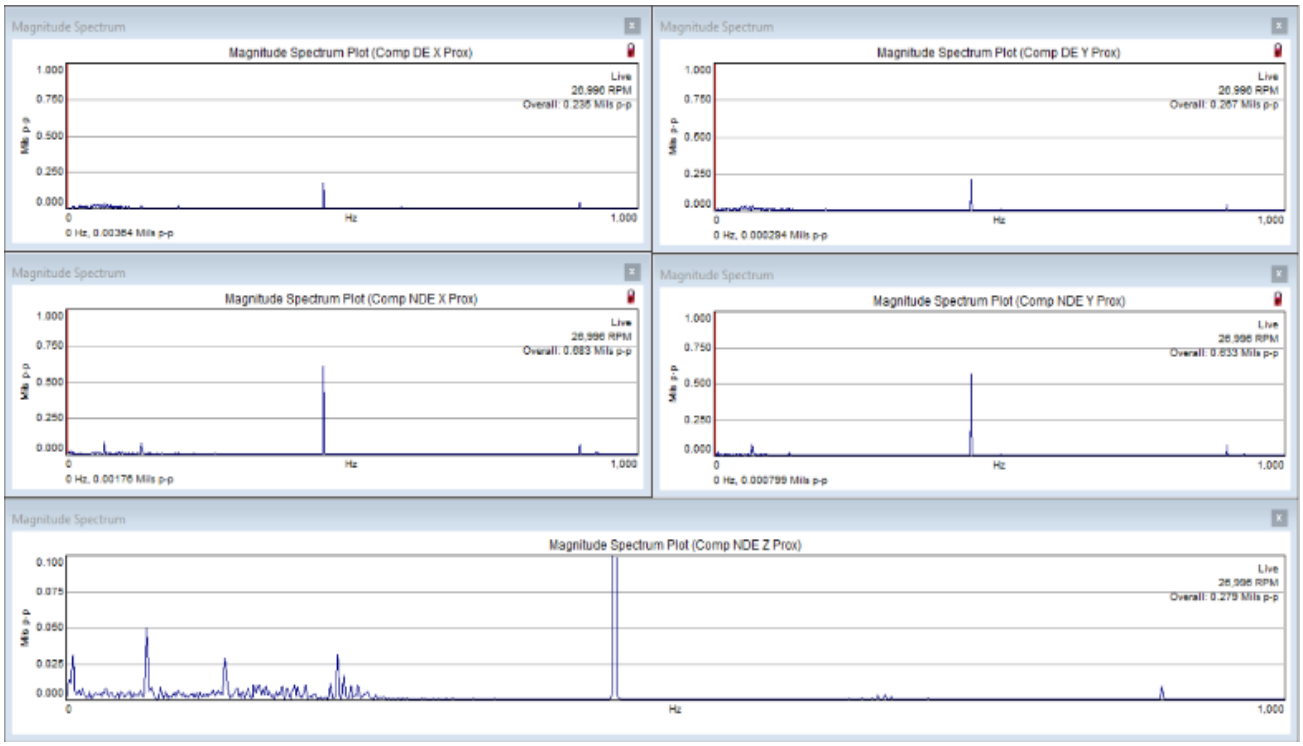

Figure 21 - 20 bar Test - Vibration Plots at 27,000 rpm at -10 IGV Set Point

The above detailed vibration plots show the overall vibrations in the compressor at various operating conditions. The critical results that are shown here is that there is no amplitude difference between +10º and -10º IGV setting. This indicates that at low pressure, there is no aerodynamic influence on the rotordynamics. With successful testing at 0.3 and 2.0 MPa, the next step in the test procedure is test the compressor at full speed and full pressure suction conditions.

HIGH PRESSURE TESTING

Once the compressor completed testing at low pressures, it was time to move into high pressure testing (>80 bar). Rather than increasing pressure incrementally, with sCO_2, it is important to ensure that you are operating above the critical point to avoid two phase flow in the system. For a high speed compressor, two phase flow can lead to high vibrations and possibly catastrophic damage to equipment. The safer option is to start above 8.3 MPa and guarantee that testing occurs with supercritical flow. For future testing after an overnight pressurized hold, the compressor would be run at low speed in the two phase region with no heat rejection to warm up the loop and bring it up to pressure without the need to add mass.

Similar to initial low pressure testing, the compressor was ramped up slowly to monitor bearing vibrations and bearing temperatures. While journal bearing temperatures should not be much different than the original testing, the thrust bearing temperatures need to be monitored closely, especially as the compressor is throttled. With higher pressure loads, the accuracy of the thrust balance calculations will be validated. Sudden changes in rotor position and increased temperature on a single thrust bearing would indicate a thrust imbalance. For the thrust bearings in this application, the design load is 9,600 N (2,150 lbf). The balance piston diameter is around 100 mm (3.94”), and if the design was off by less than 2 mm (0.08”) at maximum pressure operation, the thrust bearings would see forces above the design load. Vibrations and bearing temperatures are shown in Figure 22 through Figure 23.

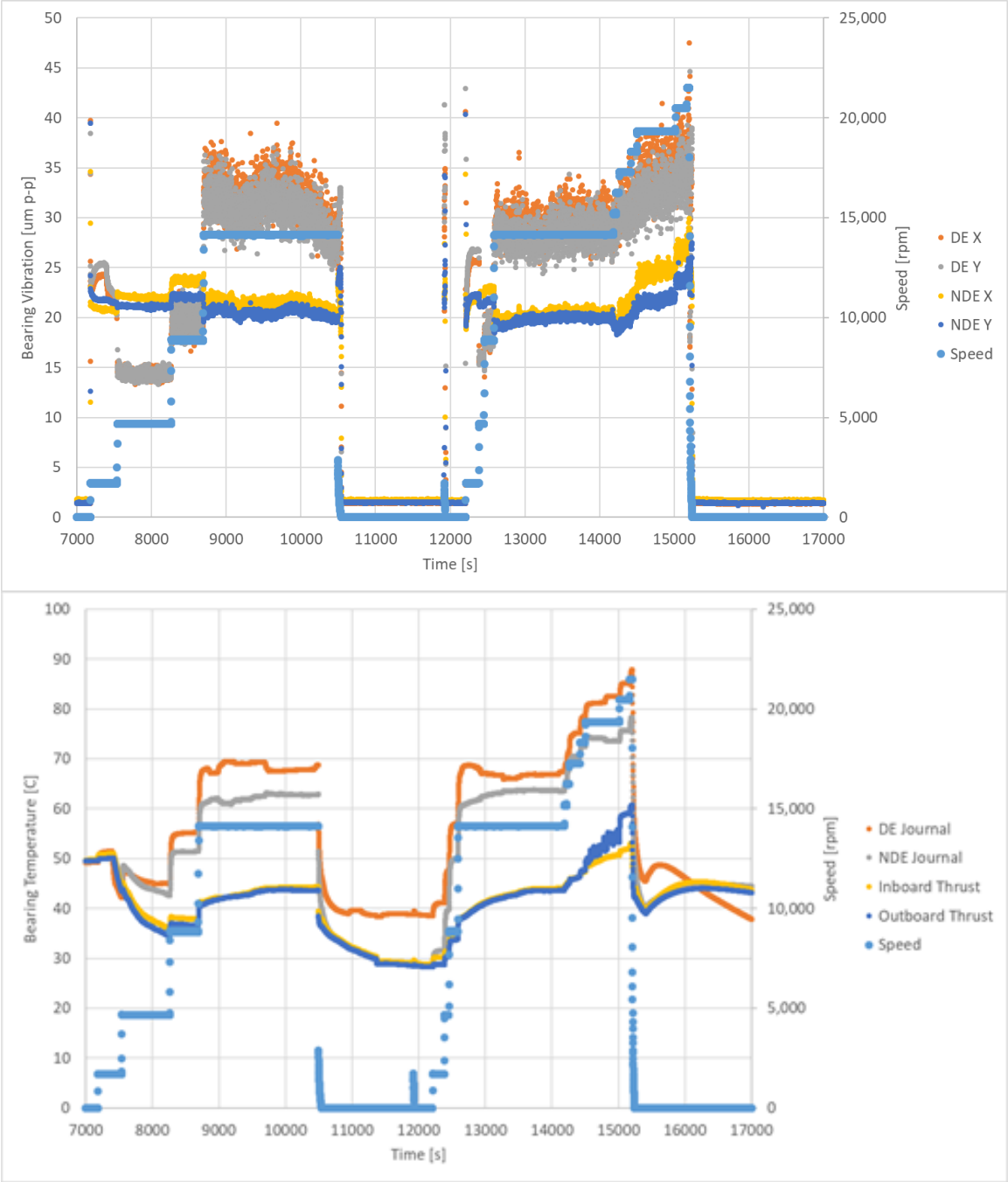

Figure 22 - High Pressure Test - Bearing Vibrations (top) and Bearing Temperatures (bottom) Compared to Speed

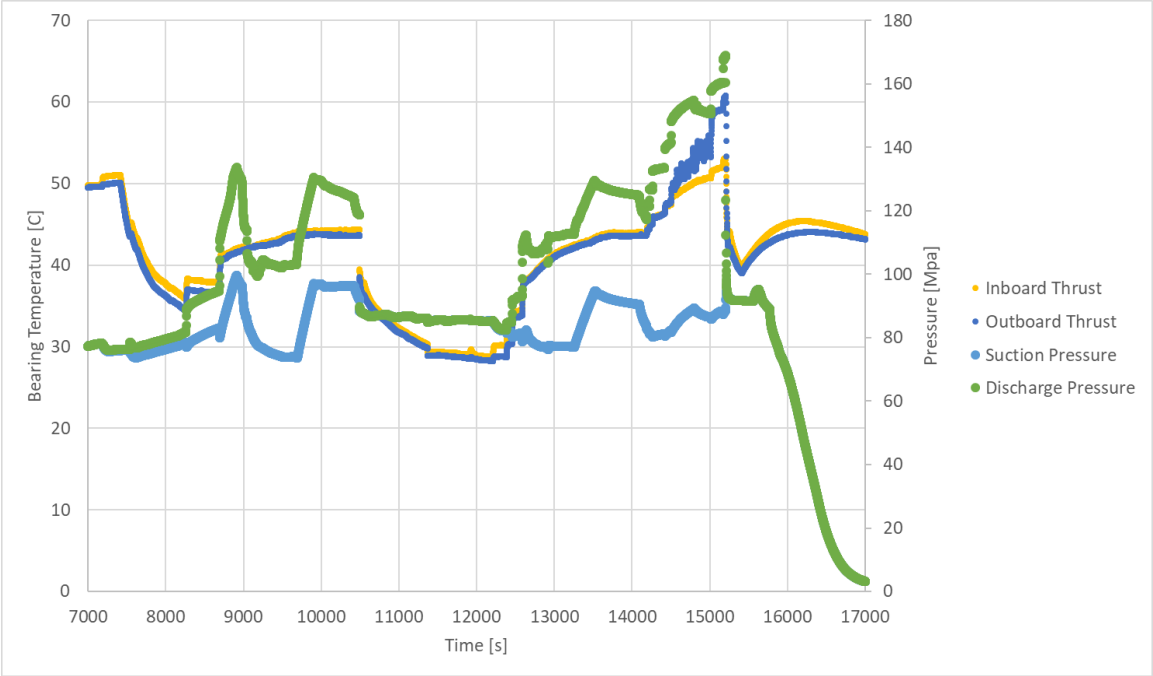

Figure 23 - High Pressure Test - Thrust Bearing Temperatures and Operating Pressure

The main thing to call attention to in the above charts is the higher vibrations seen at sCO_2 operating conditions. These vibrations prevented the compressor from operating up to full speed with the higher suction densities. Two tests were looked at to verify the source of the excitation: throttling the compressor and varying suction density. By throttling the compressor, discharge pressure is increased which will move the compressor closer to its design point and also increase pressure differential and flow across the balance piston, leading to increased damping. In terms of thrust bearing temperatures, it is important to note that as pressure was increased and speed was held constant, there was no increase in thrust bearing temperatures. The thrust bearing temperature rise along with pressure rise shown in Figure 23 is lined up more directly with increase in speed, which is expected. Figure 24 through Figure 29 show bearing vibration spectra through the high pressure testing and how it compares to low pressure testing.

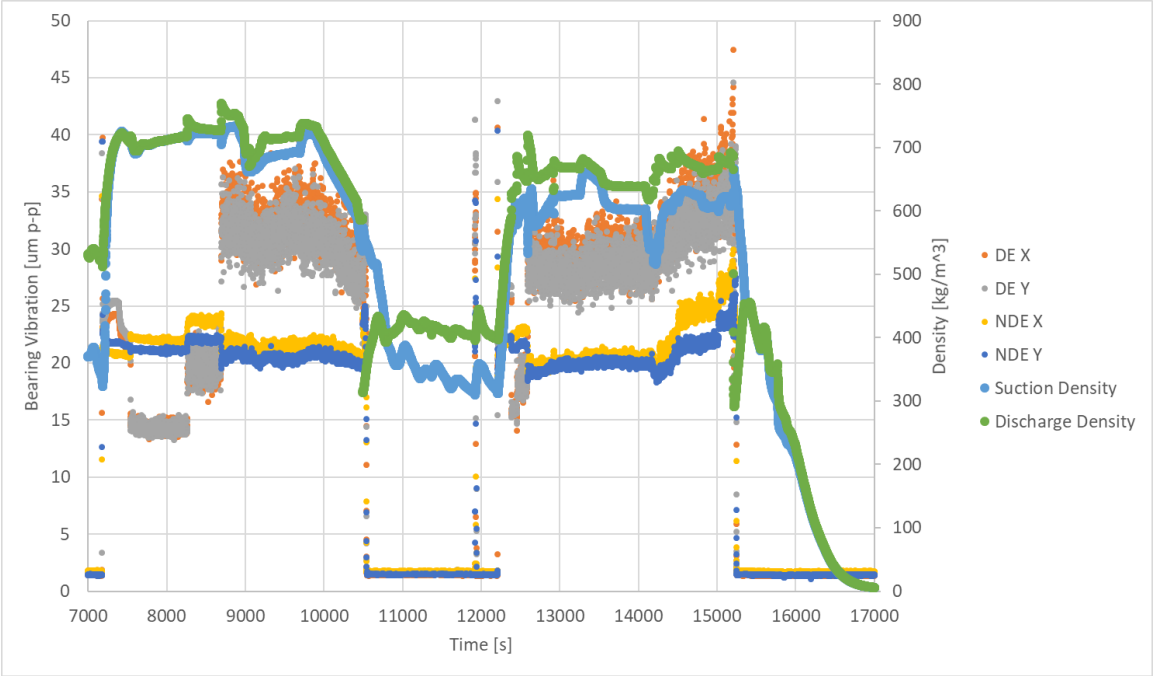

Figure 24 - High Pressure Test - Bearing Vibration and Flow Density

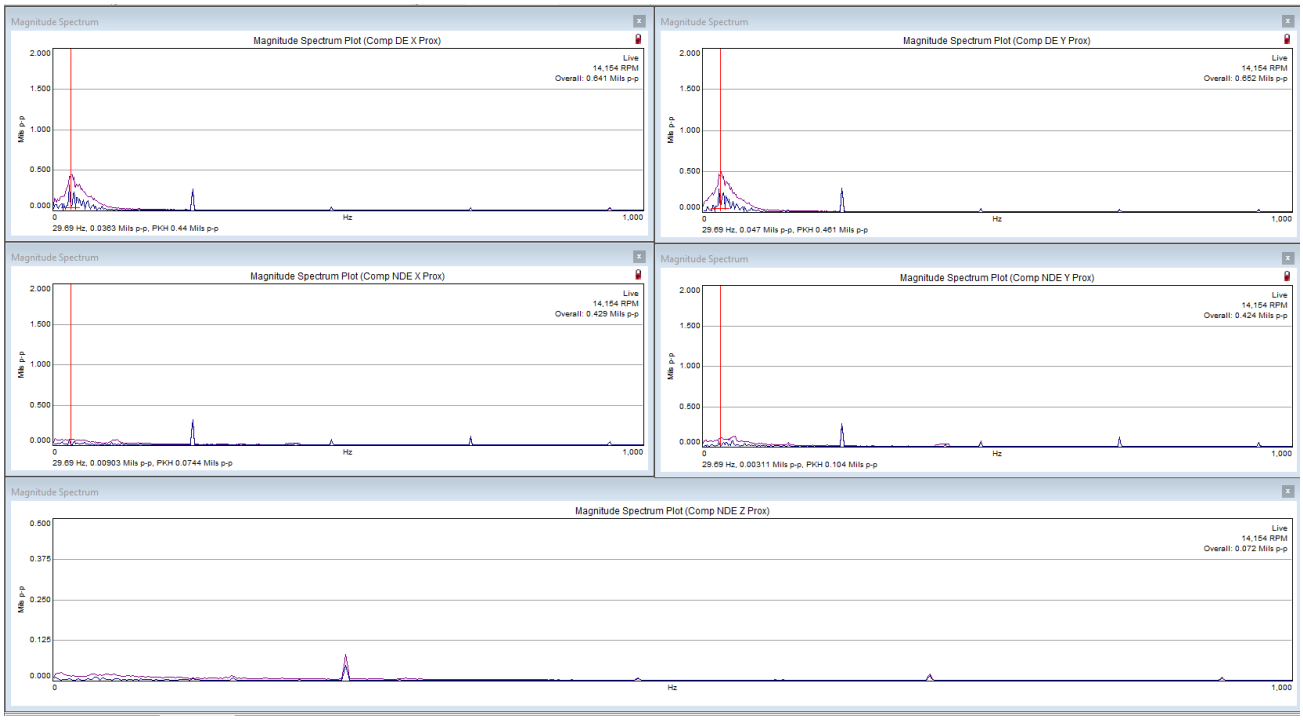

Figure 25 - Bearing Vibrations at 14,000 rpm with a Suction Density of 586 kg/m³

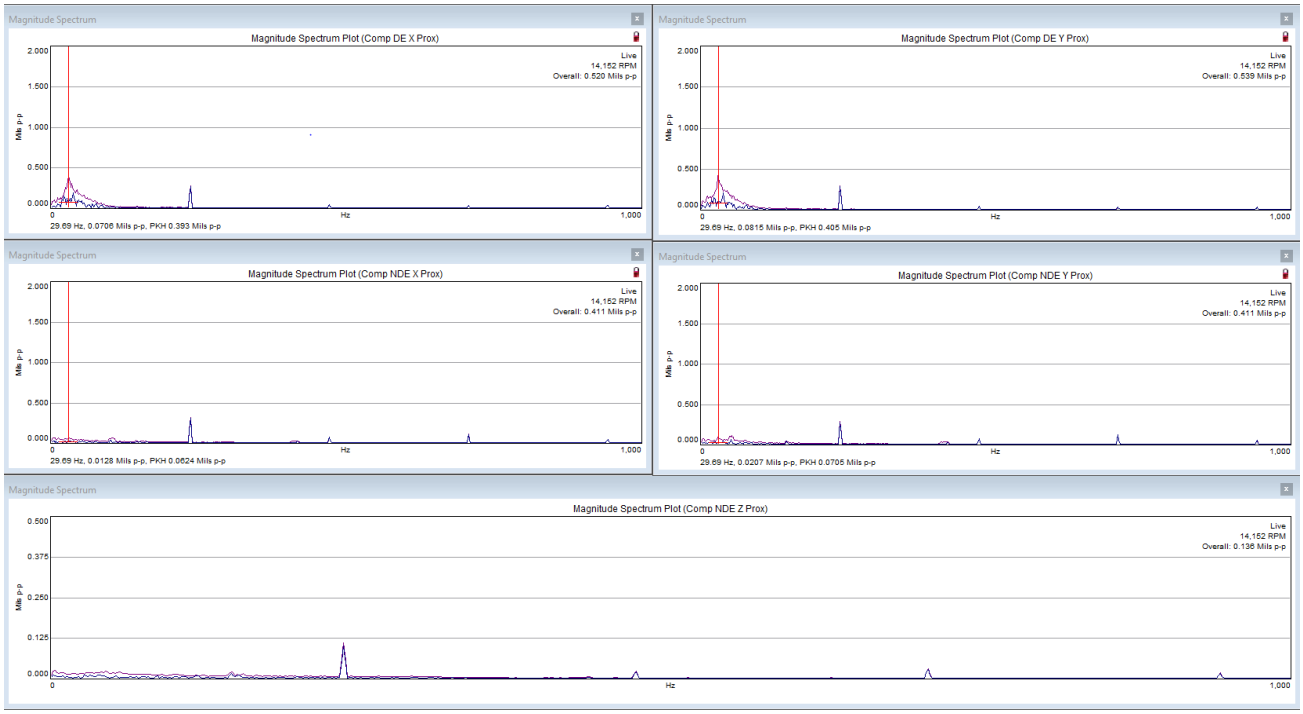

Figure 26 - Bearing Vibrations at 14,000 rpm with a Suction Density of 325 kg/m³

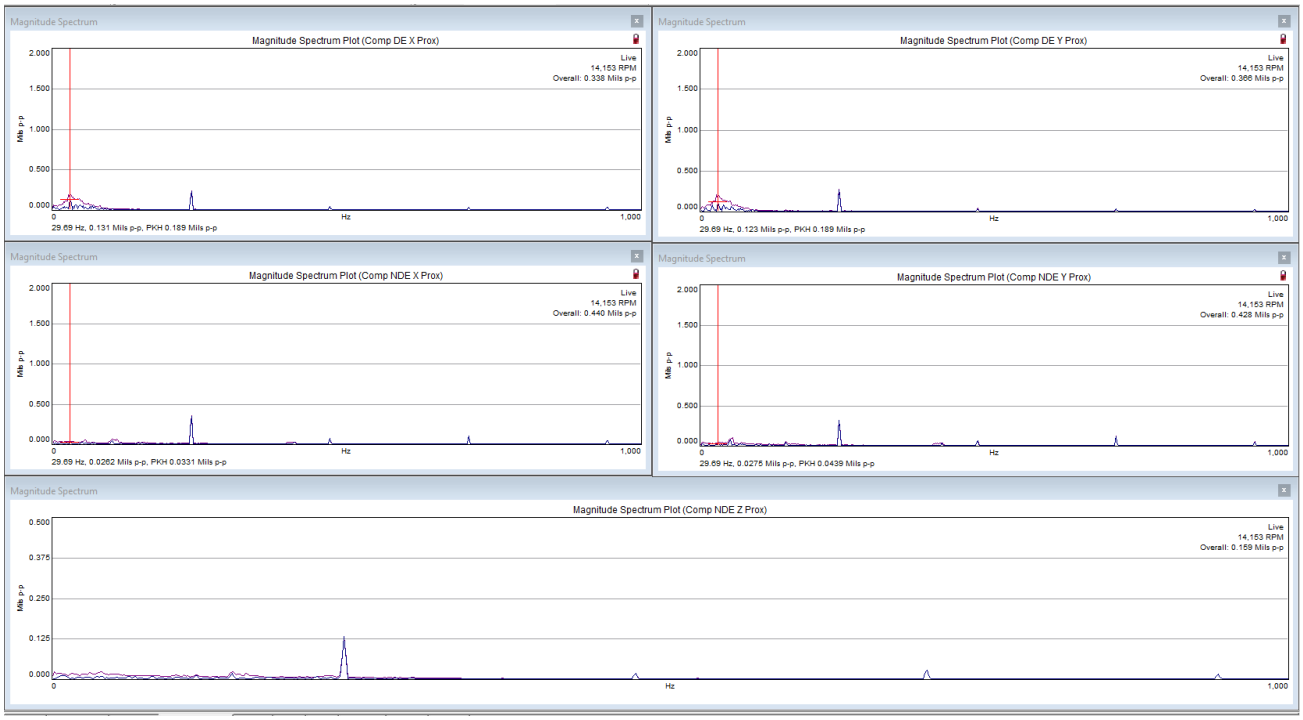

Figure 27 - Bearing Vibrations at 14,000 rpm with a Suction Density of 276 kg/m³

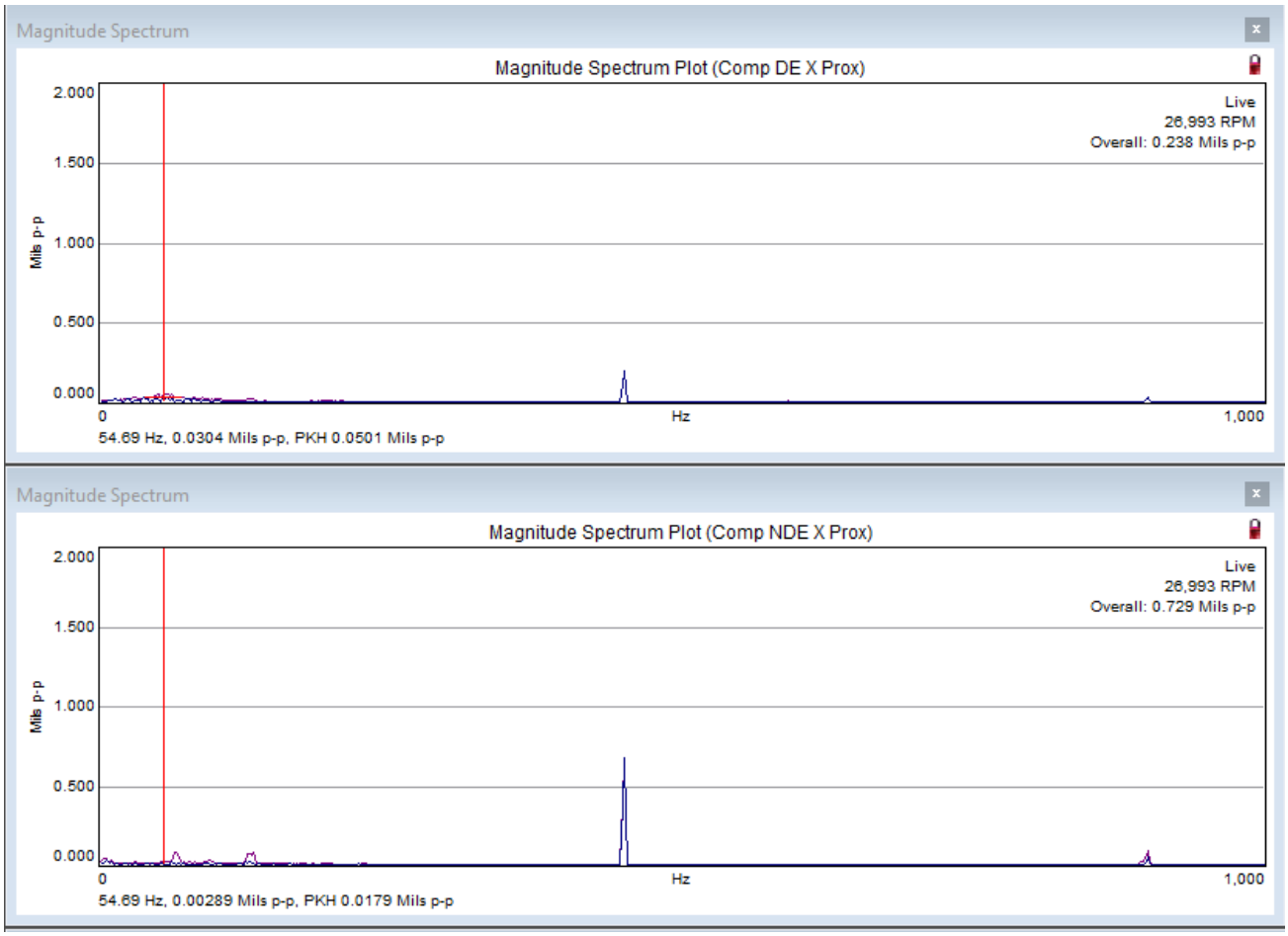

Figure 28 - Bearing Vibrations at 27,000 rpm at 2.0 MPa Suction

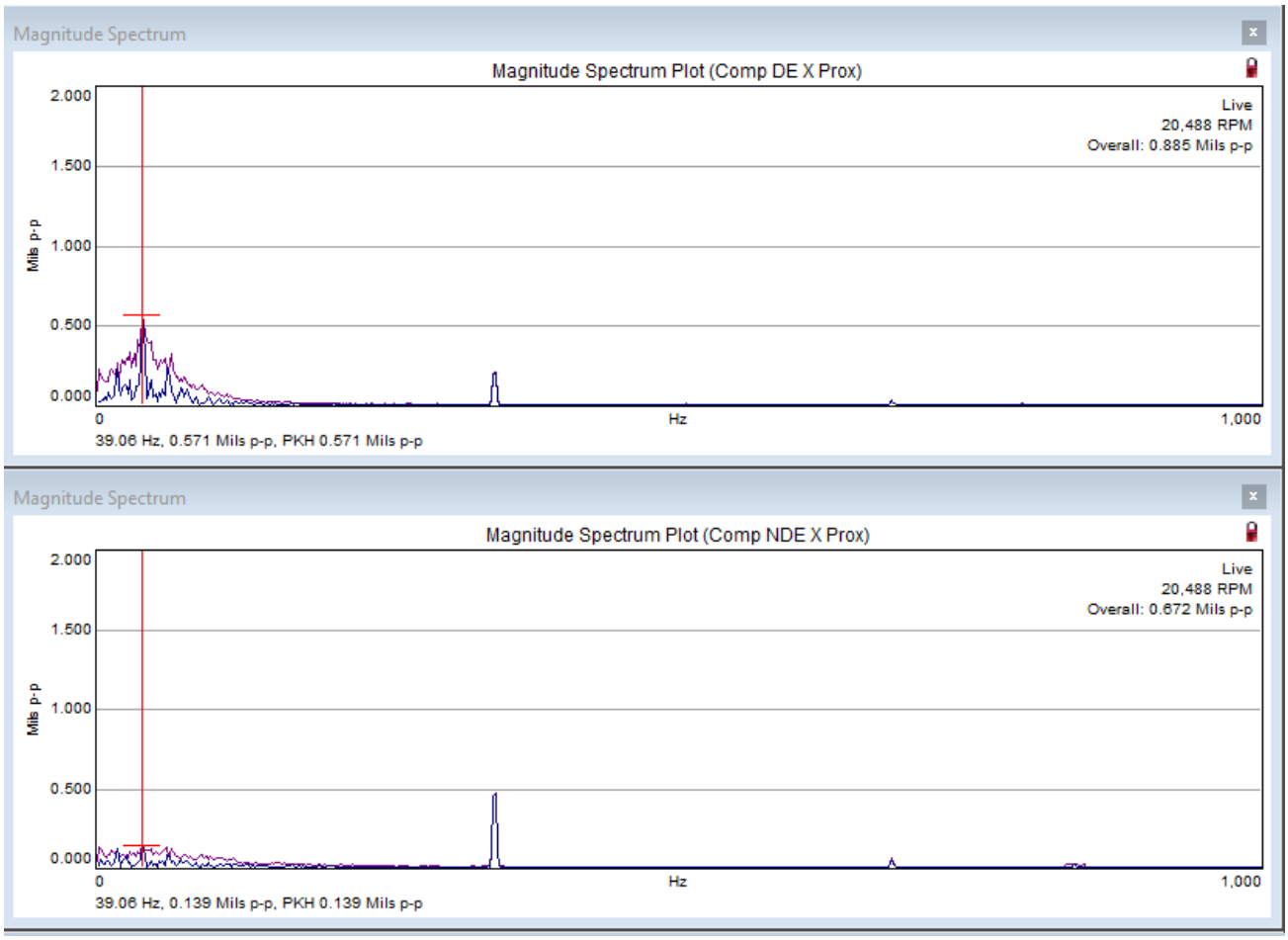

Figure 29 - Bearing VIbrations at 20,500 rpm at 8.5 MPa Suction

When looking at overall vibrations, the primary difference between high pressure and low pressure testing is the increase in subsynchronous vibration. The synchronous vibration between the two cases is very close, indicating no issue with the balance of the rotor, but that there are some low frequency broadband vibrations that are well below the predicted natural frequencies of the rotor. Due to the broadband nature of the vibration, it was determined that it was not a classic rotordynamic instability at the first mode but rather a forced excitation from the fluid. The comparison of suction density to bearing vibrations shows a direct relation. When density is decreased by 50%, the bearing vibrations are also reduced by 50%. When compared to low pressure testing, there is little to no subsynchronous vibration. For the 14,000 rpm testing, there is no change in synchronous vibrations as suction density is reduced. With the SFD design used in the journal bearings, around 1/3 of the motion in the rotor was being seen in the motion of the SFD and 2/3 in the bearing clearance. Because of this, alarm and trip limits were increased by 50% to 53.3 µm (2.1 mils) and 64.7 µm (2.5 mils). With this increase in vibration limits, 21,500 rpm was reach at supercritical conditions. However, there was a vibration trip at that speed, not allowing for full speed operation.

After review of the rotordynamics analysis, it was determined that there was a manufacturing flaw in the balance piston seal. Two important plots to look at for the increased stability due to the balance piston hole pattern seal are shown in Figure 30 and Figure 31. The balance piston did not have a taper machined into it, which is required to achieve positive damping on the system at these low frequencies. Without the taper, once the compressor was throttled, the balance piston would have a diverging taper which would lead to low stiffness and negative damping. Even though the rotor did not go unstable, the unsteady fluid forces from the high density fluid was causing significant broadband subsynchronous vibration.

In addition to the balance piston issue, it is important to note that the IGV angle was manually set to +10, which is the set point for hot day operating conditions at 50°C (122°F) compressor suction. The +10 was chosen since it leads to the highest volume flow and was the design configuration with the IGVs closest to pure radial.

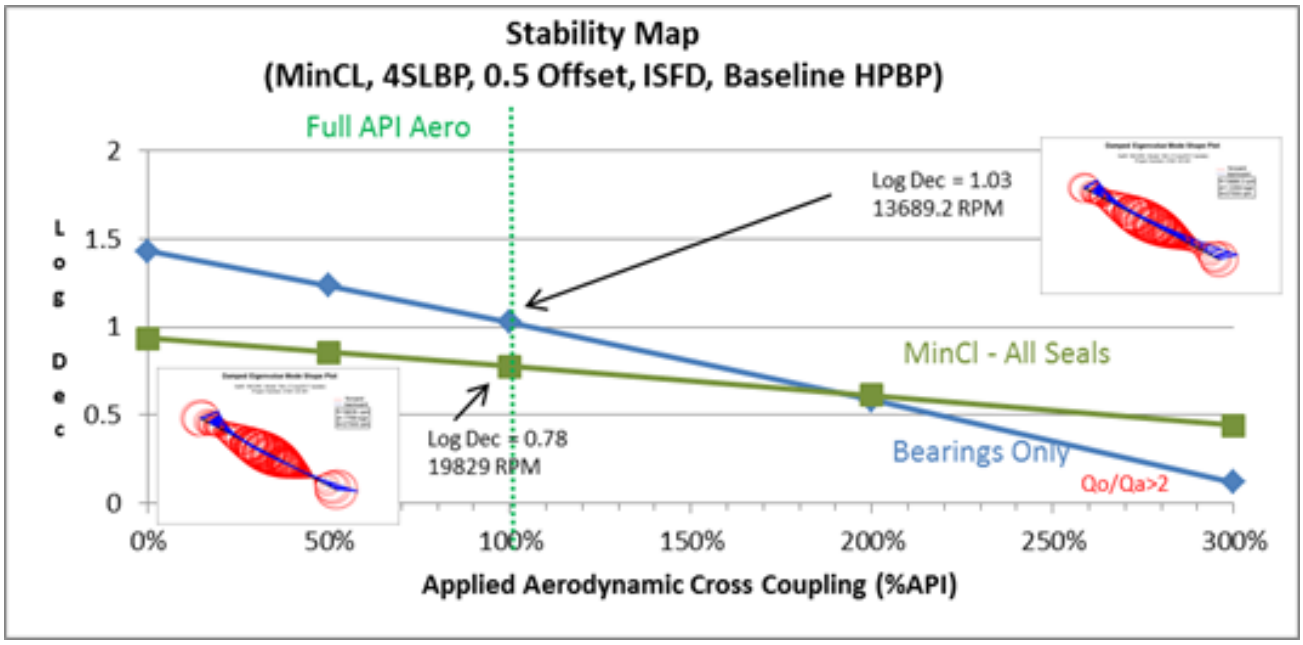

Figure 30 - Stability Map - Log Dec vs Applied Aerdynamic Cross Coupled Stiffness

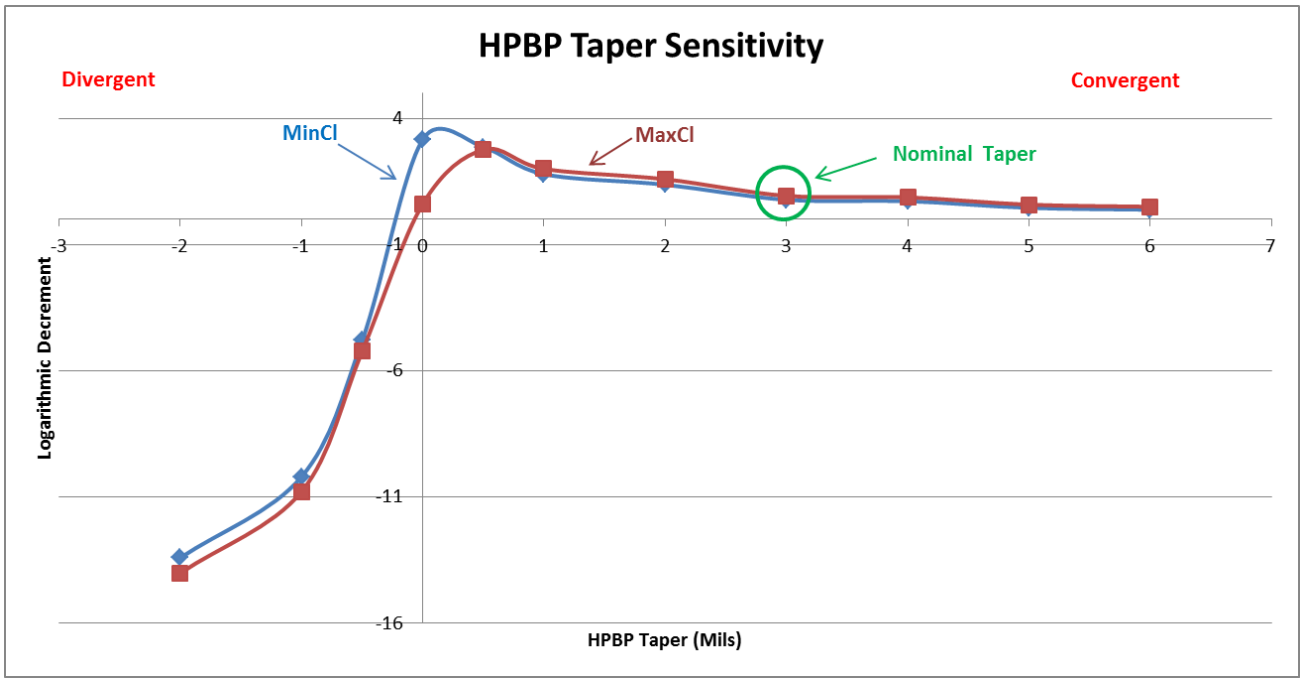

Figure 31 - Balance Piston Taper Study

The balance piston was remade with the correct taper and installed into the compressor for continued testing to see if the proper taper would solve the vibration issues that were seen in the initial round of high pressure testing. Results are shown in Figure 32 and Figure 33.

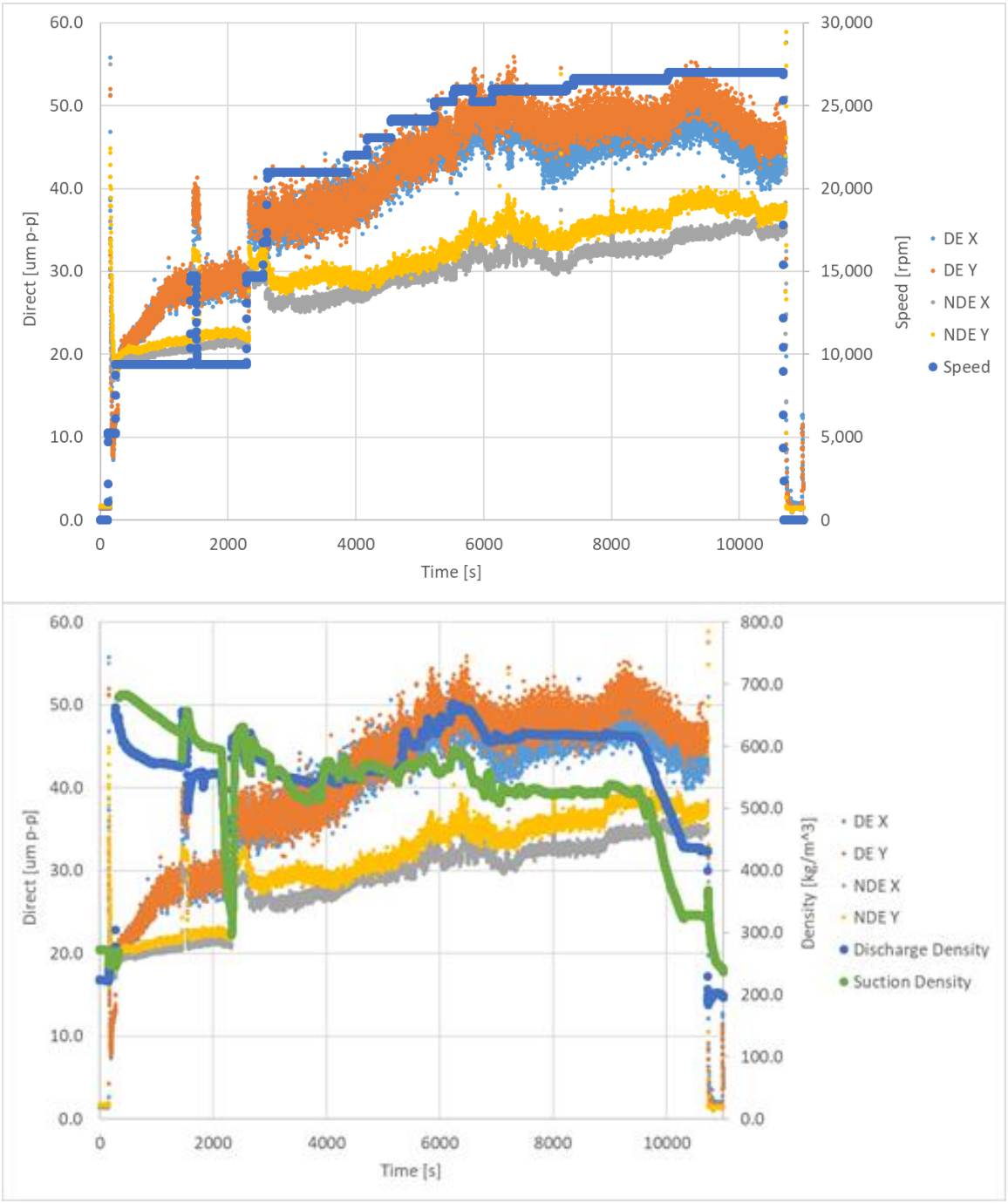

Figure 32 - Full Speed and High Pressure Test - Bearing Vibrations and Speed (top) and Bearing Vibrations and Flow Density (bottom)

Figure 33 - Full Speed and High Pressure Test - Bearing Vibrations and Fluid Pressure (top) and Bearing Temperatures and Fluid Pressure (bottom)

With the balance piston correction, the compressor was able to achieve full speed at 36ºC (97ºF) and ~8.5 MPa (1,232 psi), close to the nominal design point of 35ºC (95ºF) and ~8.5 MPa (1,232 psi). While the subsynchronous vibration decreased significantly, the vibrations were hovering around the alarm at 26,500 rpm. The vibrations were lowered by increasing suction temperature and reducing suction density. An increase in temperature of 1ºC (~2ºF) reduced the density by 7% and reduced the vibration enough to achieve design speed. Once design speed was achieved, vibrations were still hovering around alarm so suction density was continually reduced as 50ºC (122ºF) suction temperature was approached. The data shows that as the suction temperature was increased, the overall vibrations on the DE bearings ware decreasing directly with suction density. However, due to other issues, there was an internal trip (unrelated to vibration) that lead to shutting down of the machine and completed the current round of testing. Figure 34 and Figure 35 show compressor vibration spectra at 26,500 rpm and 27,000 rpm including peak-hold averaging. While the peak subsynchronous vibration was less than 7 µm p-p (0.26 mils p-p), the sum of the broad band frequencies is adding about 25 µm (1 mil) to the overall vibration.

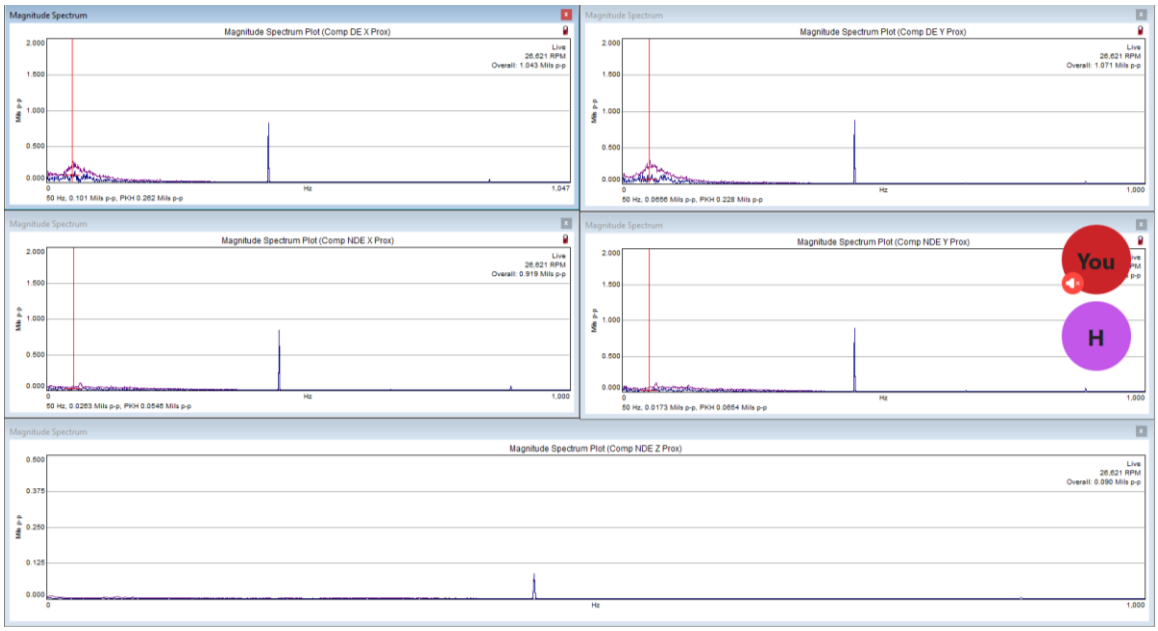

Figure 34 - Bearing Vibrations at 26,500 rpm at 35°C Suction Temperature

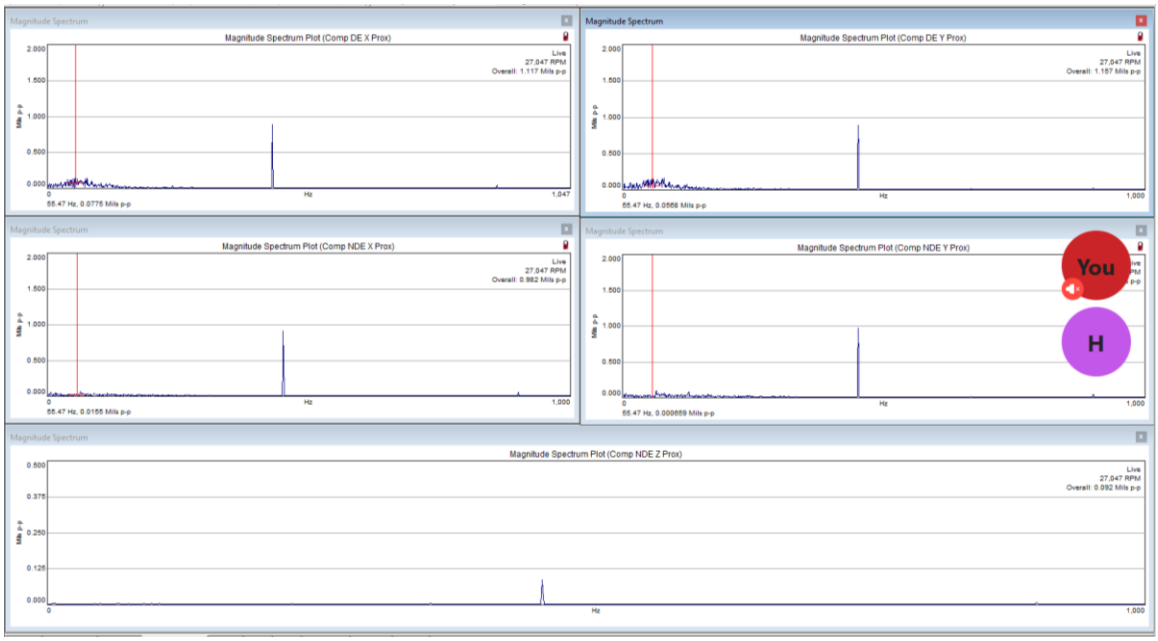

Figure 35 - Bearing Vibrations at 27,000 rpm at 36°C Suction Temperature

CONCLUSIONS

For the current round of testing, the compressor was successfully operated up to full speed and successfully compressed sCO_2. However, higher than desired vibrations were seen even after corrections to the design were made. Further design changes and rotordynamics are being evaluated further improve the vibrations to allow for successful performance testing. Further testing will include performance testing at three design points for hot day (50°C [122°F]), nominal day (35°C [95°F]), and potentially cold day (20°C [68°F]) or near to it at three difference IGV angles and two different speeds. One of the main challenges for this compressor is its need to compress efficiently over a wide range of operating conditions based on potential suction conditions during various times of the year. At a constant operating pressure of 8.5 MPa (1,233 psi), this would be a 3X swing in density from cold day to hot day. To reduce the density swing to 2X, compressor suction would be increased to around 10.0 MPa (1,450 psi), which still keeps design pressures relatively low for the loop.

At each of these points, there will be a fixed IGV set point to obtain performance maps that will then be used to validate CFD models. In addition, the performance data will be compared with low pressure performance data obtained early on in this testing. For future

manufactured compressors, this will allow for low pressure validation of designs without the need to proof test a compressor at supercritical conditions. Despite the many design and testing challenges, the program successfully developed and tested the highest density, high-speed centrifugal compressor published to date in the literature and incorporated movable geometry with discharge pressures of 25.0 MPa (3,600 psi).

While this testing was specific for the RCBC sCO_2 power applications, the challenges in efficiently compressing a highly dense fluid (60% of water) with a high-speed compressor are applicable to every application involving the compression of sCO_2. Due to its low compression head near the dome, sCO_2 has the potential to reduce power consumption in CCS and EOR applications to reduce overall operating costs and lead to higher overall efficiency of Natural Gas Combined Cycle (NGCC) and Pulverized Coal (PC) power plants with carbon capture.

REFERENCES

[1] Moore, J.J., Camatti, M., Smalley, A.J., Vannini, G.V., Vermin, L.L., 2006, Investigation of a Rotordynamic Instability in a High Pressure Centrifugal Compressor Due to Damper Seal Clearance Divergence, 7th International Conference on Rotor Dynamics, September 25-28, 2006, Vienna, Austria.

[2] Lambruschini, F., Liese, E., Zitney, S., and Traverso, A., 2016, "Dynamic Model of a 10 MW Supercritical CO_2 Recompression Brayton Cycle," *ASME Turbo Expo 2016: Turbomachinery Technical Conference and Exposition*, Seoul, South Korea.

[3] Bryant, J., Saari, H., and Zanganeh, K., 2011, "An Analysis and Comparison of the Simple and Recompression Supercritical CO_2 Cycles," *Supercritical CO_2 Power Cycle Symposium*, Boulder, Colorado, United States.

[4] McClung, A., Smith, N., Allison, T., and Tom, B., 2018, "Practical Considerations for the Conceptual Design of an sCO_2 Cycle," *6th International Supercritical CO_2 Power Cycles Symposium*, Pittsburgh, Pennsylvania, United States.

[5] McClung, A., Smith, N., Allison, T., and Tom, B., 2018, "Practical Considerations for the Conceptual Design of an sCO_2 Cycle," *6th International Supercritical CO_2 Power Cycles Symposium*, Pittsburgh, Pennsylvania, United States.

[6] Moore, J.J., Evans, N., Brun, K., Kalra, C., 2015, "Development of 1 MWe Supercritical CO_2 Test Loop," *Proceedings of the ASME Turbo Expo*, Paper #GT2015-43771, June 15-19, 2015, Montreal, Quebec, Canada.

[7] Hexemer, M, 2014, "Supercritical CO_2 Brayton Recompression Cycle Design and Control Features to Support Startup and Operation," *The 4th International Symposium – Supercritical CO_2 Power Cycles: Technologies for Transformational Energy Conversion*, Pittsburgh, Pennsylvania, USA.

[8] Spadacini, C., Pesatori, E., Centemeri, Lazzarin, N., Macchi, R., and Sanvito, M., 2018, "Optimized Cycle and Turbomachinery Configuration for an Intercooled, Recompressed sCO_2 Cycle," *The 6th International Supercritical CO_2 Power Cycles. Symposium*, Pittsburgh, Pennsylvania, United States

[9] Noall, J. and Pash, J., 2014, "Achievable Efficiency and Stability of Supercritical CO_2 Compression Systems," *Supercritical CO_2 Power Cycle Symposium*, Pittsburgh, Pennsylvania, United States.

[10] Monge, B., Sanchez, D., Savill, M., and Sanchez, T., 2014, "Exploring the Design Space of the sCO_2 Power Cycle Compressor," *The 4th International Symposium – Supercritical CO_2 Power Cycles*, Pittsburg, Pennsylvania, United States.

[11] Wacker, C. and Dittmer, R, 2014, "Integrally Geared Compressors for Supercritical CO_2," *The 4th International Symposium – Supercritical CO_2 Power Cycles*, Pittsburgh, Pennsylvania, United States.

[12] Schuster, S., Benra, F., and Brillert, D., 2016, "Small Scale sCO_2 Compressor Impeller Design Considering Real Fluid Conditions," *The 5th International Symposium – Supercritical CO_2 Power Cycles*, San Antonio, Texas, United States.

[13] Del Greco, A. and Tapinassi, L., 2013, "On the Combined Effect on Operating Range of Adjustable IGVs and Variable Speed in Process Multistage Centrifugal Compressors," *ASME Turbo Expo 2013: Turbine Technical Conference and Exposition*, San Antonio, Texas, USA.

[14] Cich, S., Moore, J., Mortzheim, J., and Hofer, D, 2018, "Design of a Supercritical CO_2 Compressor for use in a 10 MWe Power Cycle," *The 6th International Supercritical CO_2 Power Cycles Symposium*, Pittsburgh, Pennsylvania, United State.

[15] Tan, J., Qi, D., and Wang, R., 2010, "The Effect of Radial Inlet on the Performance of Variable Inlet Guide Vanes in Centrifugal Compressor Stage,: *ASME Turbo Expo 2010: Power for Land, Sea, and Air*, Glasgow, UK.

[16] Sezal, I., Chen, N., Aalburg, C., Gadamsetty, R., Erhard, W., Del Greco, A., Tapinassi, L., and Lang, M., 2016, "Introduction of Circumferentially Non-uniform Variable Guide Vanes in the Inlet Plenum of a Centrifugal Compressor for Minimum

Losses and Flow Distortion," *Journal of Turbomachinery*, September 2016, Vol. 138.

[17] Ertas, B., Delgado, A., and Moore, J., 2018, "Dynamic Characterization of an Integral Squeeze Film Bearing Support Damper for a Supercritical CO_2 Expander," *Journal of Engineering for Gas Turbines and Power*.

[18] Cich, S., Moore, J., Towler, M., Mortzheim, J., and Hofer, D., 2019, "Loop Filling and Start Up with a Closed Loop sCO_2 Brayton Cycle," *ASME 2019 Turbo Expo*, Phoenix, Arizona, United States.

ACKNOWLEDGEMENTS

This material is based upon work supported by the Department of Energy, Office of Energy Efficiency and Renewable Energy (EERE), under Award Number DE-EE0007109. This report was prepared as an account of work sponsored by an agency of the United States Government. Neither the United States Government nor any agency thereof, nor any of their employees, makes any warranty, express or implied, or assumes any legal liability or responsibility for the accuracy, completeness, or usefulness of any information, apparatus, product, or process disclosed, or represents that its use would not infringe privately owned rights. Reference herein to any specific commercial product, process, or service by trade name, trademark, manufacturer, or otherwise does not necessarily constitute or imply its endorsement, recommendation, or favoring by the United States Government or any agency thereof. The views and opinions of authors expressed herein do not necessarily state or reflect those of the United States Government or any agency thereof